Petroleum Systems and Geologic Assessment of Oil and Gas in the San Joaquin Basin Province, California

Chapter 12

A Four-Dimensional Petroleum Systems Model for the San Joaquin Basin Province, California

By Kenneth E. Peters, Leslie B. Magoon, Carolyn Lampe[1], Allegra Hosford Scheirer, Paul G. Lillis, and Donald L. Gautier

Contents

Abstract

A calibrated numerical model depicts the geometry and three-dimensional (3-D) evolution of petroleum systems through time (4-D) in a 249 x 309 km (155 x 192 mi) area covering all of the San Joaquin Basin Province of California. Model input includes 3-D structural and stratigraphic data for key horizons and maps of unit thickness, lithology, paleobathymetry, heat flow, original total organic carbon, and original Rock-Eval pyrolysis hydrogen index for each source rock. The four principal petroleum source rocks in the basin are the Miocene Antelope shale of Graham and Williams (1985; hereafter referred to as Antelope shale), the Eocene Kreyenhagen Formation, the Eocene Tumey formation of Atwill (1935; hereafter referred to as Tumey formation), and the Cretaceous to Paleocene Moreno Formation. Due to limited Rock-Eval/total organic carbon data, the Tumey formation was modeled using constant values of original total organic carbon and original hydrogen index. Maps of original total organic carbon and original hydrogen index were created for the other three source rocks. The Antelope shale was modeled using Type IIS kerogen kinetics, whereas Type II kinetics were used for the other source rocks.

Four-dimensional modeling and geologic field evidence indicate that maximum burial of the three principal Cenozoic source rocks occurred in latest Pliocene to Holocene time. For example, a 1-D extraction of burial history from the 4-D model in the Tejon depocenter shows that the bottom of the Antelope shale source rock began expulsion (10 percent transformation ratio) about 4.6 Ma and reached peak expulsion (50 percent transformation ratio) about 3.6 Ma. Except on the west flank of the basin, where steep dips in outcrop and seismic data indicate substantial uplift, little or no section has been eroded. Most

[1]IES GmbH, Integrated Exploration Systems, Ritterstrasse 23, 52072 Aachen, Germany

petroleum migration occurred during late Cenozoic time in distinct stratigraphic intervals along east-west pathways from pods of active petroleum source rock in the Tejon and Buttonwillow depocenters to updip sandstone reservoirs. Satisfactory runs of the model required about 18 hours of computation time for each simulation using parallel processing on a Linux-based cluster.

Introduction and Geologic Setting

The San Joaquin Basin Province of central California is an asymmetrical structural trough that contains up to about 10 km (32,800 ft) of Mesozoic and Cenozoic (mostly Miocene and younger) sedimentary rocks deposited in a forearc basin setting between a trench in the west and a magmatic arc in the east (fig. 12.1). The boundaries of the province are defined to the east by the Sierra Nevada plutonic complex, to the west by the San Andreas Fault, to the north by the Stockton Arch, and to the south by the Tehachapi-San Emigdio Mountains. The axis of the basin is parallel to and near its western margin. Localized uplift resulted in minor erosion in the southernmost part of the basin. Major uplift occurred on the west side of the basin as the basin margin changed from a convergent to a transform boundary. Subsidence dominated the Cenozoic Era in the San Joaquin Basin. Most sedimentary rocks originated in marine settings, except along the eastern margin of the basin where the Cenozoic rocks contain mixtures of marine and nonmarine input (Bartow and McDougall, 1984). Deep-water marine organic-rich shaly source rocks and turbidite sandstones characterize the central areas of the basin. The geologic history of this forearc basin is further discussed by Callaway (1971; 1990), Gautier and others (this volume, chapter 2) and Johnson and Graham (this volume, chapter 6).

The term "petroleum systems modeling" rather than "basin modeling" is used in this paper to describe 3-D calibrated numerical modeling through geologic time that may involve multiple petroleum systems. Petroleum systems models recreate basin history, but their primary goal is to describe petroleum systems, including the extent and timing of petroleum generation, migration, and accumulation. The term "4-D petroleum systems modeling" refers specifically to the three spatial dimensions and the component of time.

A complete 4-D model of the San Joaquin Basin is useful because such models provide more quantitative information on the complex elements and processes characterizing petroleum systems than conventional geologic studies (see, for example, Welte and others, 1997). Four-dimensional models can serve as research tools to evaluate geological scenarios or make predictions that can be tested by drilling. They represent a powerful means to identify or rank those elements or processes of petroleum systems that require more study. Finally, 4-D models provide a systematic way to archive data and interpretations that might otherwise be lost.

Few 4-D petroleum systems models of the San Joaquin Basin have been published. Welte and others (1997) completed a 4-D simulation for a portion of the San Joaquin Basin extending from north of Westhaven to the Stockton Arch (fig. 12.1). They used a low, constant heat flow of 46 mW/m^2 through geologic time for the western flank of their study area. Calculated and observed calibration parameters agreed in key wells on the western flank. However, simulation of key wells on the eastern flank demonstrated that the constant, low heat flow did not lead to acceptable calibrations. Their work further indicated that heat flow in the east must have been as high as 67 mW/m^2 prior to 7 million years ago, and as low as 38 mW/m^2 in more recent times, presumably due to heating events associated with the Sierra Nevada magmatic arc. The transition to rapidly decreasing heat flow coincided with an abrupt change in crustal configuration that occurred about 7 to 8 Ma in the study area, caused by the northward migration of the Mendocino triple junction. This northward migration converted the subduction zone into a transform margin during the late Cenozoic Era (Atwater, 1970).

The 4-D model of the San Joaquin Basin Province developed in this study contains generalized input that precluded analysis of the model results on a field-by-field basis. However, this model provides valuable insights into the extent and timing of petroleum generation and directions of petroleum migration. Results and interpretations from the model were used in the U.S. Geological Survey (USGS) 2003 assessment of undiscovered oil and gas resources in the San Joaquin Basin Province (Gautier and others, 2004; Gautier and others, this volume, chapter 2). The results described in this paper were obtained from an evolving 4-D model that allowed revisions to be made as more data became available.

Objectives

The objectives of our 4-D petroleum systems modeling of the San Joaquin Basin Province were to (1) map and better define the levels of thermal maturity within pods of active petroleum source rock, (2) determine the timing of initial and peak expulsion of petroleum for each pod of active source rock, and (3) identify pathways for petroleum migration from the source-rock pods to the traps.

Total Petroleum System

Total petroleum-system processes include the generation, migration, and accumulation of petroleum, as well as trap formation (Magoon and others, this volume, chapter 8). Four-dimensional petroleum systems modeling is a systematic method to better understand petroleum occurrence because it accounts for each of these processes and includes available data on the essential geologic elements necessary for petroleum accumulations (Magoon and Dow, 1994). In the San Joaquin Basin, these geologic elements include four Meso-

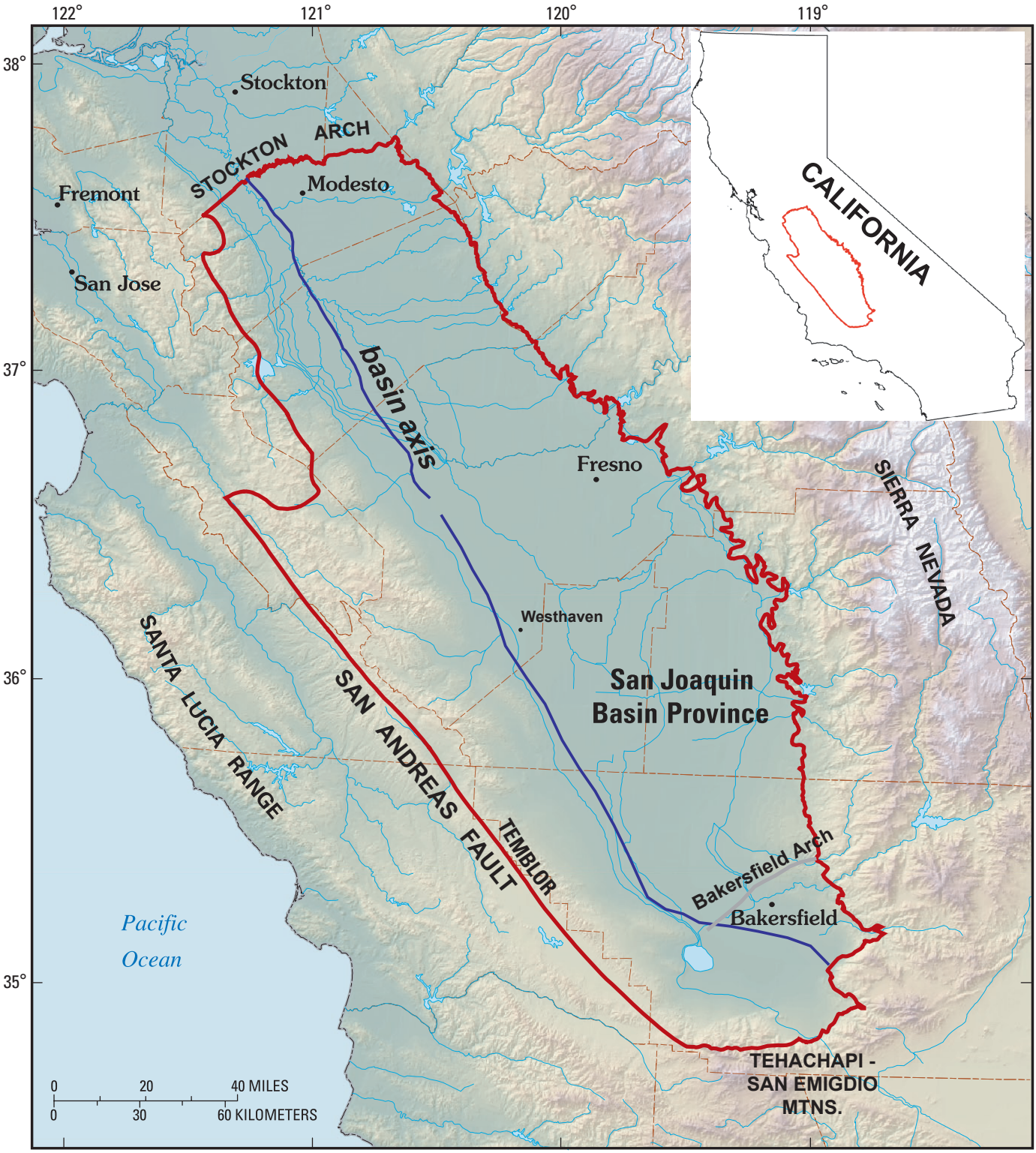

Figure 12.1. Map of the San Joaquin Basin shows the outline of the study area (San Joaquin Basin Province; red line), basin axis, and key geographic features discussed in the text. Inset shows the outline of the study area within California. The basin axis and the Bakersfield Arch are mapped on the three-dimensional geologic model of the San Joaquin Basin (see Hosford Scheirer, this volume, chapter 7). The basin axis is defined on the top of the Temblor Formation in the southern two-thirds of the basin and on the top of the Ragged Valley silt of Hoffman (1964) in the northern third of the basin.

zoic- to Cenozoic-aged source-rock units, reservoir rocks, seal rocks, and overburden rocks. Examples of useful information obtained using the total petroleum system concept include the maximum geographic extent of the petroleum system and the critical moment for each source rock. The critical moment is a snapshot in time that best depicts the generation, migration, and accumulation of petroleum. The critical moment is chosen at the discretion of the investigator but must occur between the times of peak expulsion and depletion of the generative potential of the source rock (Magoon and Dow, 1994). Details of the petroleum system elements and processes in the San Joaquin Basin are discussed below.

Petroleum Systems Model Development

Four-dimensional modeling of the geologic history of petroleum systems includes simulation of petroleum generation, migration, and accumulation through discrete time steps. Each time step in a petroleum systems model consists of a framework of calculations that are required to generate the input for the next simulation time step. For example, the calculated temperature at each time step during burial of a source rock is required to determine the volumes of generated petroleum. Likewise, calculated pore pressure is needed to evaluate the timing and extent of expulsion (primary migration). The time- and space-dependent differential transport equations needed for modeling and the finite element methods used for their solutions are beyond the scope of this paper but are documented in the literature (Zienkiewicz, 1977; Aziz and Settari, 1979).

Figure 12.2 shows the process workflow for our 4-D petroleum systems modeling of the San Joaquin Basin Province. The model was constructed and run using PetroMod® software version 8.1 manufactured by Integrated Exploration Systems (IES), Inc. PetroMod® employs "hybrid migration modeling," which integrates full 3-D Darcy flow with flowpath migration to allow reasonable calculation times for large models without the need to reduce the number of nodes in the model space (Hantschel and others, 2000).

Our hybrid-flow 4-D model for the San Joaquin Basin Province covers an area of 249 x 309 km (155 x 192 mi) and involves 24 stratigraphic layers with more than 1.8 million grid cells (appendix). Computations involving such large models would be impractical without the speed and convenience offered by parallel computing using Beowulf cluster technology. A Beowulf cluster links many inexpensive off-the-shelf personal computers to allow supercomputer performance by parallel processing (Gropp and others, 2003). Our Linux-based Beowulf cluster consists of four compute nodes, each with two processors (for a total of 8 physical and 8 virtual processors), plus a master node. Using hyperthreading, the Beowulf cluster can complete a simulation of the model with x and y grid resolution of 1 km^2 (0.386 miles^2) in about 18 hours.

4-D Model Input Parameters

PetroMod® uses deterministic forward modeling, in which basin processes are modeled from the past to the present using inferred starting conditions (Welte and others, 1997). The basin history is subdivided into an uninterrupted sequence of depositional, nondepositional, or erosional events of specified age and duration. Numerical values are required for all input parameters (fig. 12.2). Input data include gridded surfaces of buried rock units derived from seismic and well-log interpretations, ages of units, present and past rock-unit thicknesses, lithologies and physical properties of units, porosity, permeability, and various boundary conditions, such as present and past water depths, basal heat flow, and surface or sediment-water interface temperatures. Geochemical data, such as the type and amount of organic matter in the source rocks and the kinetics for the conversion of kerogen (particulate organic matter in sedimentary rocks that is insoluble in organic solvents) to petroleum are also required.

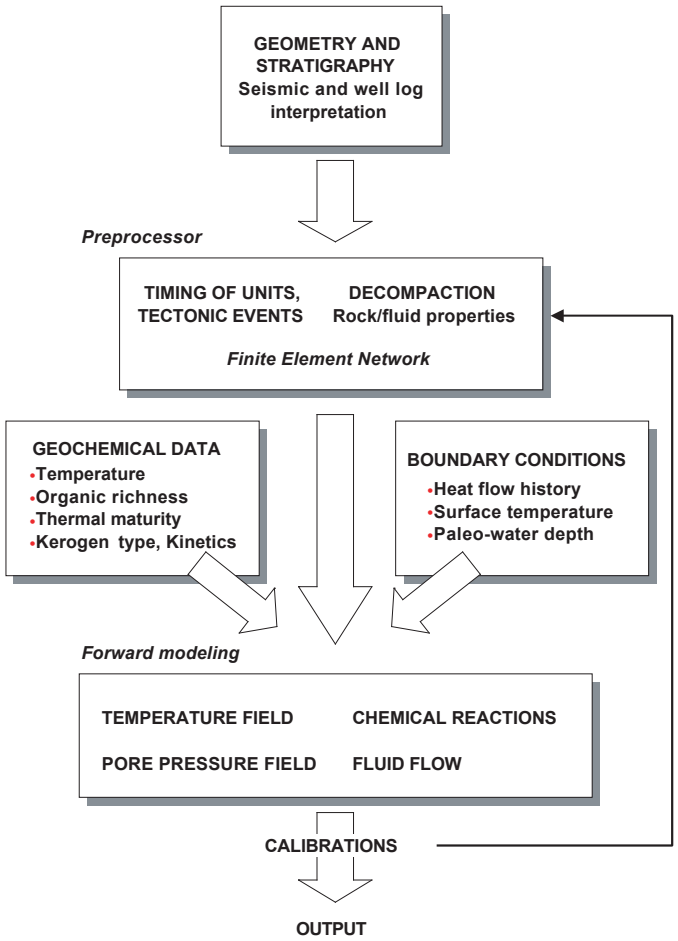

Figure 12.2. Process workflow diagram for four-dimensional (4-D) numerical modeling of the geohistory of petroleum systems. We use the term "4-D petroleum systems modeling" to refer to numerical modeling of the generation, migration, and accumulation of petroleum in three spatial dimensions through geologic time.

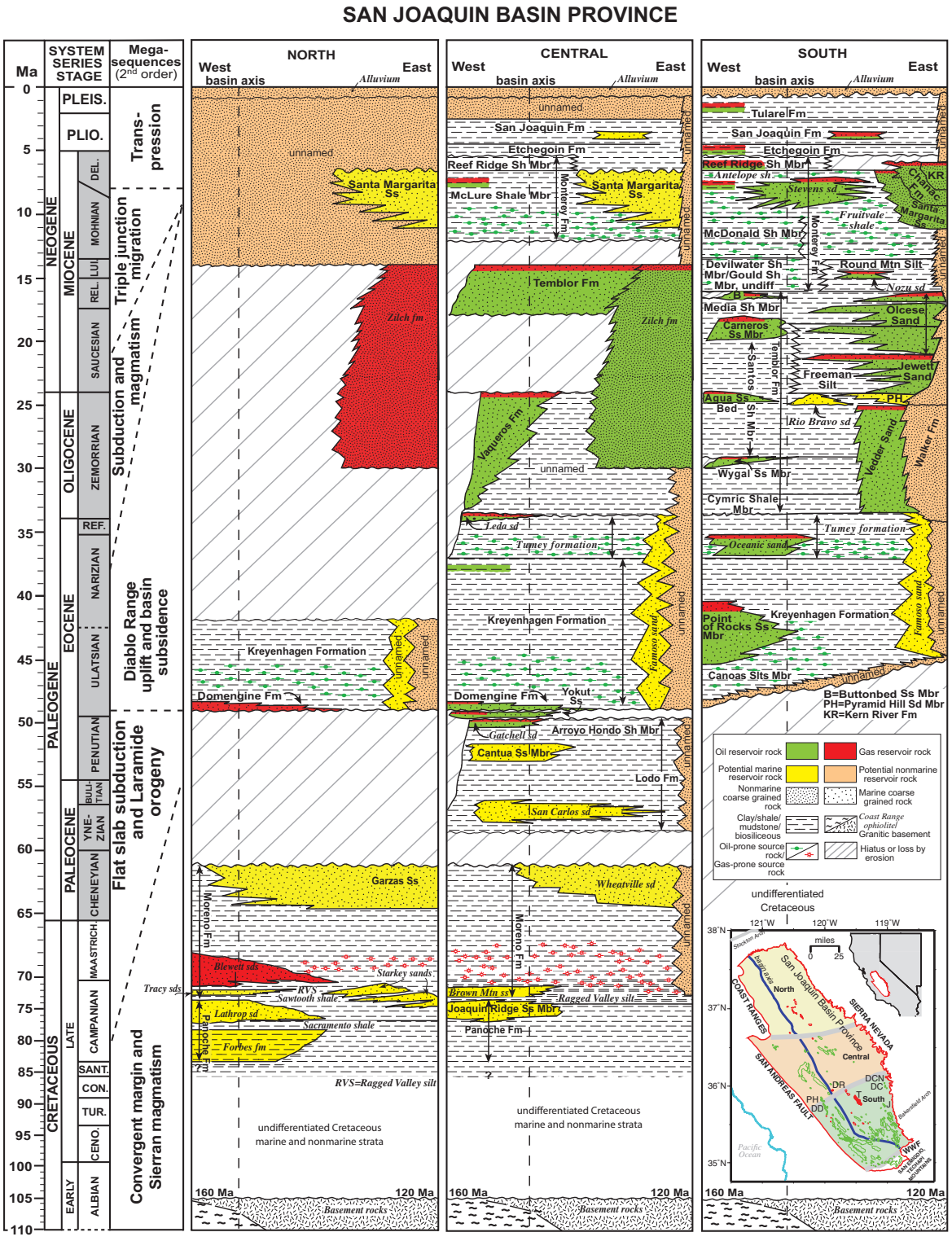

Figure 12.3. San Joaquin Basin Province stratigraphy showing hydrocarbon reservoir rocks and potential hydrocarbon source rocks. See Hosford Scheirer and Magoon (this volume, chapter 5) for complete explanation of the figure. Formation names in italics are informal and are defined as follows (in approximate age order): Forbes formation of Kirby (1943), Sacramento shale and Lathrop sand of Callaway (1964), Sawtooth shale and Tracy sands of Hoffman (1964), Brown Mountain sandstone of Bishop (1970), Ragged Valley silt, Starkey sands, and Blewett sands of Hoffman (1964), Wheatville sand of Callaway (1964), San Carlos sand of Wilkinson (1960), Gatchell sand of Goudkoff (1943), Oceanic sand of McMasters (1948), Leda sand of Sullivan (1963), Tumey formation of Atwill (1935), Famoso sand of Edwards (1943), Rio Bravo sand of Noble (1940), Nozu sand of Kasline (1942), Zilch formation of Loken (1959), Stevens sand of Eckis (1940), Fruitvale shale of Miller and Bloom (1939), and Antelope shale of Graham and Williams (1985).

Chronostratigraphic Units

Clastic rocks that range from coarse sandstone to siltstone and shale dominate the stratigraphic succession in the San Joaquin Basin (fig. 12.3). The backbone of our 4-D petroleum systems model is a 3-D geologic map of the San Joaquin Basin sedimentary succession prepared by Hosford Scheirer (this volume, chapter 7). This map is a digital compilation of key source rock and reservoir rock units, which consists of a series of gridded surfaces that were combined into an internally consistent geological model. Our petroleum systems model further subdivides the 3-D geologic map into 24 chronostratigraphic rock units (table 12.1, fig. 12.4). Geologic layers used for numerical modeling are best described as chronostratigraphic rather than lithologic units in so much as each layer was constructed by combining time-equivalent units into a single layer bearing the name of the dominant member. However, each layer is assigned a lithology or mixture of lithologies within PetroMod® so that facies variations are properly accounted for during modeling. Hosford Scheirer (this volume, chapter 7) describes the constituent members of each layer.

Digitally gridded subsurface maps obtained from various sources were prepared with uniform 1-km (3,280-ft) cell dimensions. A petroleum company, which chose to remain anonymous, graciously provided us with structure contour maps of key horizons mapped using in-house seismic data. These surfaces were checked for accuracy using available well logs. For example, the "N-marker," near the top of the Antelope shale (top of "nonsource," table 12.1) is a key horizon that determines the structural characteristics of many petroleum accumulations in the 4-D model.

Additional surfaces were generated using EarthVision® software and well log data obtained mainly from the California Department of Conservation, Division of Oil, Gas, and Geothermal Resources (for full references see Hosford Scheirer, this volume, chapter 7) and cross sections available from the Pacific Section of the American Association of Petroleum Geologists (PS-AAPG, 1957a,b, 1958a,b, 1959, 1989). In our San Joaquin Basin model, sedimentary rocks overlie crystalline basement rocks dating to about 106 Ma. The gridded basement surface was obtained using the digital map database of Wentworth and others (1995).

Using age constraints from several sources (Hosford Scheirer and Magoon, this volume, chapter 5), chronostratigraphic units in the model (table 12.1) were assigned beginning and ending ages of deposition. In one case, ages of a depositional hiatus were assigned. Lithologies or mixtures of lithologies were assigned to account for the lithofacies in each rock unit. PetroMod® default physical and thermal rock properties, including thermal conductivities and heat capacities, were assigned to each lithology or mixture of lithologies.

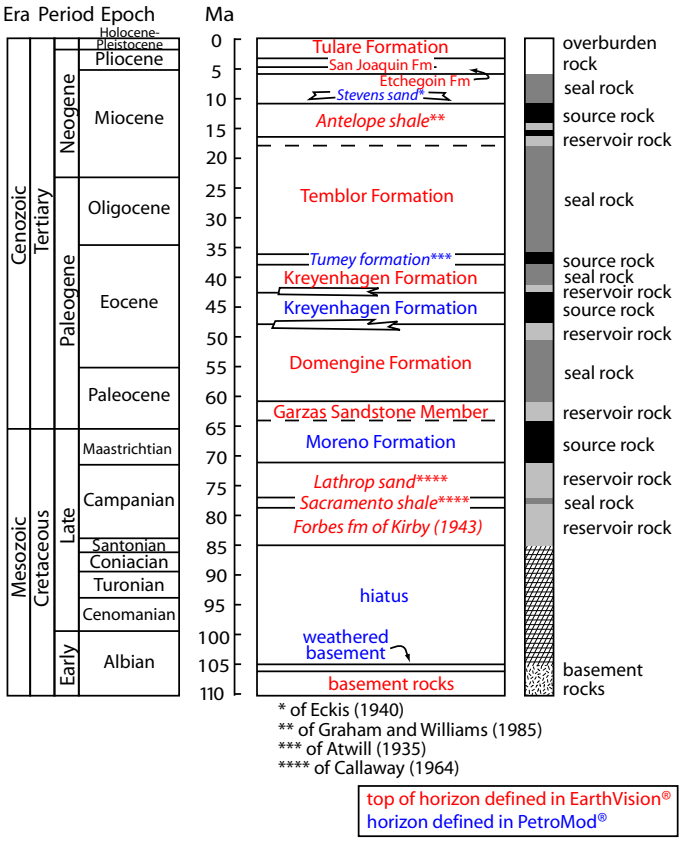

Figure 12.4. Ages of stratigraphic horizons constructed in EarthVision® from gridded seismic horizons and well-log data (Hosford Scheirer, this volume, chapter 7) and in PetroMod® version 8.1 software. The simplified chronostratigraphy in this figure was used to develop the four-dimensional (4-D) model and differs from the more detailed stratigraphy in table 12.1 and figure 12.3. Geologic layers used for numerical modeling are described as chronostratigraphic rather than lithologic units in so much as each layer combines time-equivalent units into a single layer bearing the name of the dominant member. Formation names in italics are informal. Fm, Formation; fm, formation.

Source rocks

The San Joaquin Basin contains one Mesozoic and three Cenozoic source-rock units (fig. 12.3). As discussed above, we simplified the complex stratigraphy in figure 12.3 to construct our 4-D model (table 12.1; fig. 12.4). The accompanying paper (Peters, Magoon, Valin, and Lillis, this volume, chapter 11) describes maps of the regional extent, burial depth, thickness, and original organic richness of petroleum source rocks in the basin. The source rocks include the Antelope shale, the Eocene Tumey formation, the Eocene Kreyenhagen Formation, and the Cretaceous to Paleocene Moreno Formation. For this study, the "Antelope shale" includes the McLure Shale Member of the Monterey Formation north of the Bakersfield Arch, and the Antelope shale, Fruitvale shale of Miller and Bloom (1939), and the McDonald Shale Member of the Monterey Formation to the south.

Reservoir and Seal Rocks

The 4-D model of the San Joaquin Basin is a representation that only approximates the complexity of reservoir rock and seal

rock units and traps. For example, because unconformity surfaces can be migration pathways, we assigned a uniform thickness of permeable "weathered basement" to the top 20 m (66 ft) of the comparatively impermeable basement to allow migration of petroleum along the unconformity surface. Petroleum reservoir units in our model include the Etchegoin Formation, Stevens sand of Eckis (1940; hereafter referred to as Stevens sand), Temblor Formation, Point of Rocks Sandstone Member of the Kreyenhagen Formation, Garzas Sandstone Member of the Moreno Formation, Lathrop sand of Callaway (1964), Forbes formation of Kirby (1943), and weathered basement (fig. 12.4; the table also contains references for the informal units). These units were modeled by assuming mainly sandstone lithologies (75 to 100 percent sandstone and 0 to 25 percent shale), except for the weathered basement (67 percent sandstone, 33 percent conglomerate) and the Garzas Sandstone, Temblor Formation, and Etchegoin Formation, which were modeled using mapped lithologies (courtesy of Tor Nilsen, 2003, written commun.). Seal rocks in the model result wherever low-permeability units abut against reservoir units upon superposition of the lithofacies maps (see, for example, fig. 12.5). Lithofacies maps for the Garzas Sandstone; the Tulare, San Joaquin, Etchegoin, and Domengine Formations; and the upper part of the Temblor Formation differentiate sandstone versus shale compositions in fractions of 100 percent in one of the following ratios: 100:0, 75:25, 50:50, 25:75, or 0:100. Underburden units below the Moreno Formation source rock were modeled using single lithologies (for example, 100 percent sandstone or 100 percent shale).

Traps

Structural traps evident in the gridded surfaces account for many accumulations in the model, particularly near and to the west of the basin axis (for example, Lost Hills field). Some stratigraphic traps in the model resulted from the lateral pinchout of permeable reservoir rocks (for example, Stevens sand and Point of Rocks Sandstone) into less permeable seal rocks. Where stratigraphically trapped petroleum accumulations occur in the basin, especially to the east of the basin axis, it was necessary to manually insert shale facies or impermeable faults into some reservoir units to trap migrating oil in the 4-D model.

4-D Model Boundary Conditions

Paleobathymetry

Regional water depth during deposition of each rock unit was estimated by using the paleobathymetry maps of Beyer and Bartow (1987) and Reid (1995). Some controversy exists as to the usefulness of benthic Foraminifera for this purpose. For example, Bloch (1991) questioned the assumption of Bandy and Arnal (1969) that certain Miocene Foraminifera occupied the same bathymetric zones as their modern equivalents. Figure 12.5 gives examples of the paleobathymetry (Tulare Formation) and lithology (San Joaquin Formation) input for two formations in the model.

Temperature and Heat Flow

The temperature of the sediment-water interface was calculated through time using an option in PetroMod® that relates geologic age and mean surface paleotemperature based on plate tectonic reconstructions to present-day latitude (fig. 12.6). These temperature values are subsequently corrected by PetroMod® for water depth. For example, 4 km (13,000 ft) of water depth yields a sediment-water interface temperature of 4°C, regardless of paleolatitude.

PetroMod® and similar software require present-day and paleo-heat flow to reconstruct the temperature history of basins and the thermal maturation of source-rock organic matter (Welte and others, 1997). Heat flow measures the conductive component of heat transferred through the Earth's crust to the surface and is expressed in milliwatts per square meter (mW/m^2). The most common approach to determine the Earth's heat flow involves measuring temperatures in a borehole and the thermal conductivity of the rock penetrated by the borehole. The temperature measurements are used to calculate the geothermal gradient or rate of temperature change with depth. Thermal conductivity measures the ability of the rock to transport heat and is reported in watts per meter-degrees Kelvin (W/m•K). Heat flow is the product of geothermal gradient and thermal conductivity.

Figure 12.7 is a present-day surface heat flow map based on temperature and thermal-conductivity measurements from 42 locations (including shallow wells and aqueduct tunnels) in and around the San Joaquin Basin. The map is consistent with previously published studies, which indicate that heat flow is generally higher along the western than eastern side of the San Joaquin Basin (Sass and others, 1971). Calibration results for several 4-D models were compared, where each model used a different basal heat-flow map constructed by systematically altering the original input surface heat-flow grid. The best fit of modeled maturity to available maturity measurements in calibration wells was obtained by using a basal heat-flow grid that was identical to present-day surface heat flow, as discussed below.

Petroleum Generation Kinetics

The model calculations employed Type IIS kerogen kinetics determined on shale from the Monterey Formation to simulate thermal cracking of the Antelope shale source rock and Type II kinetics determined on Toarcian shale from the Paris Basin for the Tumey formation, Kreyenhagen Formation, and Moreno Formation source rocks (Behar and others, 1997). The decision to use Type II or Type IIS kinetics was based on sulfur content of crude oils that were geochemically correlated to each source-rock unit (Lillis and Magoon, 2004; Lillis and Magoon, this volume, chapter 9). However, some nonbiodegraded crude

Table 12.1. Assigned age and petroleum system element information for stratigraphic units in the 4-D petroleum systems model. The model was developed in PetroMod® using estimated ages of deposition or nondeposition events based on our simplified nomenclature for San Joaquin Basin chronostratigraphic units. Approximate event ages are based on constraints from several literature sources (Hosford Scheirer and Magoon, this volume, chapter 5). Formation names in italics are informal and referenced as follows: Antelope shale of Graham and Williams (1985), Stevens sand of Eckis (1940), Tumey formation of Atwill (1935), Ragged Valley silt of Hoffman (1964), Tracy sands of Hoffman (1964), Sawtooth shale of Hoffman (1964), Lathrop sand of Callaway (1964), Sacramento shale of Callaway (1964), and Forbes formation of Kirby (1943).

Age of Interval (Era/Epoch)			PetroMod® Stratigraphic Unit	Deposition (Ma)		Hiatus (Ma)		Petroleum System Element
				From	To	From	To	
Cenozoic	Tertiary	Pliocene to Pleistocene	Tulare Formation	3.5	0.0			Overburden-reservoir rock
		Pliocene	San Joaquin Formation	4.8	3.5			
		Miocene to Pliocene	Etchegoin Formation	6.0	4.8			
		Miocene	*Antelope shale*, nonsource	11.0	6.0			
			Antelope shale (top)	15.5	11.0			Source rock
			Stevens sand	15.5	15.5			Reservoir rock
			Antelope shale (bottom)	16.5	15.5			Source rock
			Temblor Formation	18.5	16.5			Reservoir rock
		Oligocene to Miocene	Temblor Formation	36.0	18.5			Seal rock
		Eocene to Oligocene	*Tumey formation*	38.0	36.0			Source rock(s)
		Eocene	Kreyenhagen Formation	42.0	38.0			
			Point of Rocks Sandstone Member of Kreyenhagen Formation	43.0	42.0			Reservoir rock
			Kreyenhagen Formation	48.0	43.0			Source rock
		Paleocene to Eocene	Domengine Formation	61.0	48.0			Reservoir rock
		Paleocene	Garzas Sandstone Member of Moreno Formation	64.0	61.0			Reservoir rock
Mesozoic	Cretaceous to Paleocene		Moreno Formation	72.0	64.0			Source rock
	Cretaceous		*Ragged Valley silt*	73.0	72.0			Reservoir rock
			Tracy sands	73.5	73.0			Underburden
			Sawtooth shale	75.0	73.5			
			Lathrop sand	77.0	75.0			
			Sacramento shale	78.0	77.0			
			Forbes formation	85.0	78.0			
	Cretaceous and older		weathered basement	106.0	105.0	105.0	85.0	Basement
			fresh basement	162.0	106.0			

oils attributed to the Antelope shale source rock lack sufficient sulfur to have originated from Type IIS kerogen. High sulfur content in Type IIS kerogens, such as the phosphatic member of the Miocene Monterey Formation, may explain the tendency of these kerogens to generate petroleum at lower levels of thermal maturity than others (Orr, 1986; Peters and others, 1990; Baskin and Peters, 1992), although high oxygen content has also been implicated (Jarvie and Lundell, 2001).

The 4-D model simulates the generation of petroleum from the source rocks as two distinct fluid fractions—(1) light oil (Moreno Formation only) or medium oil (other source rocks) and (2) wet gas. The ratio of oil to wet gas is controlled by the proportion of the hydrogen index assigned to each fluid in PetroMod®.

Calibration

Calibration of the 4-D model was required to determine the timing of petroleum generation and expulsion in the San

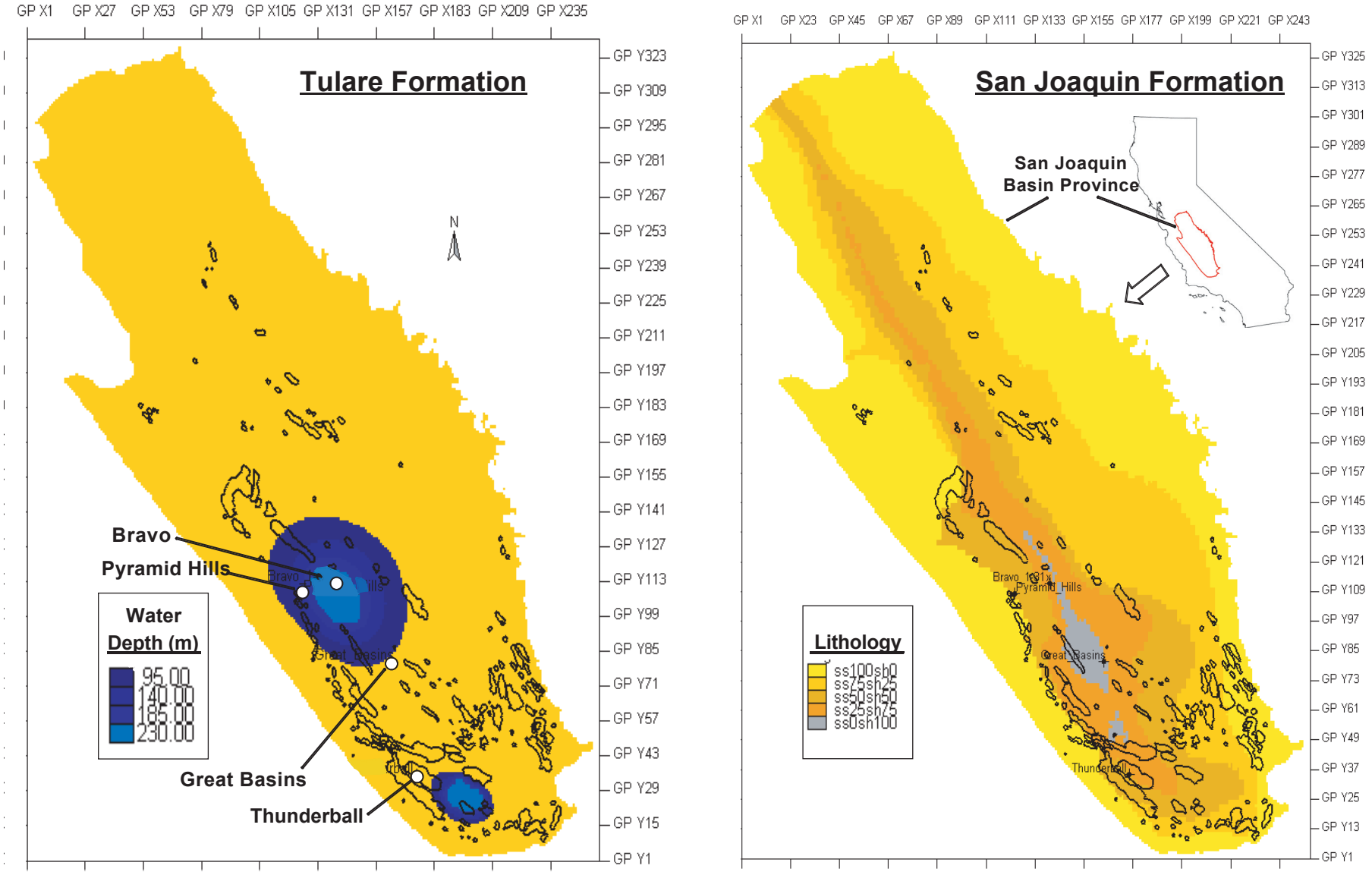

Figure 12.5. Examples of input data for the four-dimensional (4-D) petroleum systems model of the San Joaquin Basin study area. Left panel shows paleobathymetry of the Pliocene to Pleistocene age Tulare Formation (Beyer and Bartow, 1987; Reid, 1995), and right panel shows lithofacies variations in the Pliocene San Joaquin Formation (courtesy of Tor Nilsen, 2003, written commun.). The inset (right) shows the location of the study area in California. Four labeled wells were used for calibration as described in figure 12.8.

Joaquin Basin Province. Various parameters, such as heat flow, thermal and physical properties of different rock lithologies, surface temperature, and sediment deposited (burial) or eroded (uplift) can be used for calibration. However, many of these parameters, such as thermal and physical properties, are constrained within rather narrow ranges of values and cannot be significantly modified for calibration purposes. Therefore, we used heat flow as the primary model calibration parameter.

Use of at least two independent calibration tools, such as vitrinite reflectance (R_o, percent) and equilibrated or Horner-corrected bottom-hole temperatures, is recommended for reliable temperature history reconstruction (Welte and others, 1997). The 4-D model was calibrated by comparing measured vitrinite reflectance and corrected bottom-hole temperatures in selected wells with the corresponding values predicted by the model at those locations ("1-D extractions"; fig. 12.8). The model calculates vitrinite reflectance values using the "Easy%R_o" method of Sweeney and Burnham (1990).

Forward modeling of petroleum systems requires basal rather than surface heat flow as input. Basal heat flow may include heat supplied from the deep mantle, radiogenic heat from the crust, and any transient heat provided by thermal events. Our 4-D model assumes steady-state heat flow through geologic time, requiring that the surface heat flow equals heat flow from basement rocks into the sedimentary section. No thermal events supply transient heat in the model. Therefore, present-day heat flow (fig. 12.7) combined with radiogenic heat contributed by the basement rock comprise the basal

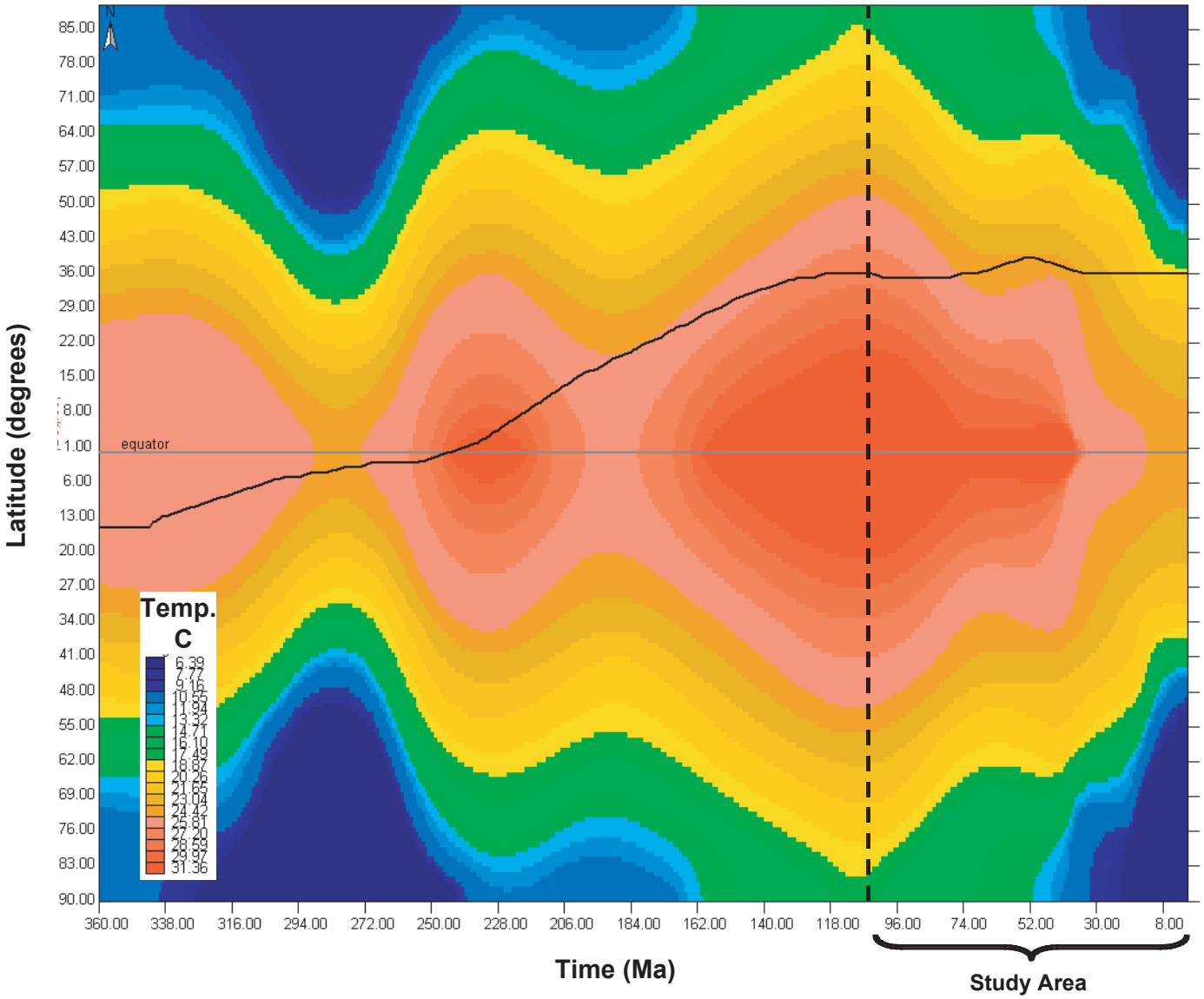

Figure 12.6. Global mean surface temperature, as a function of latitude and time, based on Wygrala (1989). The solid dark line to the right of the vertical dashed line depicts the sediment-water interface temperature during deposition of sediments in the San Joaquin Basin study area (North America, about 36° North latitude present day).

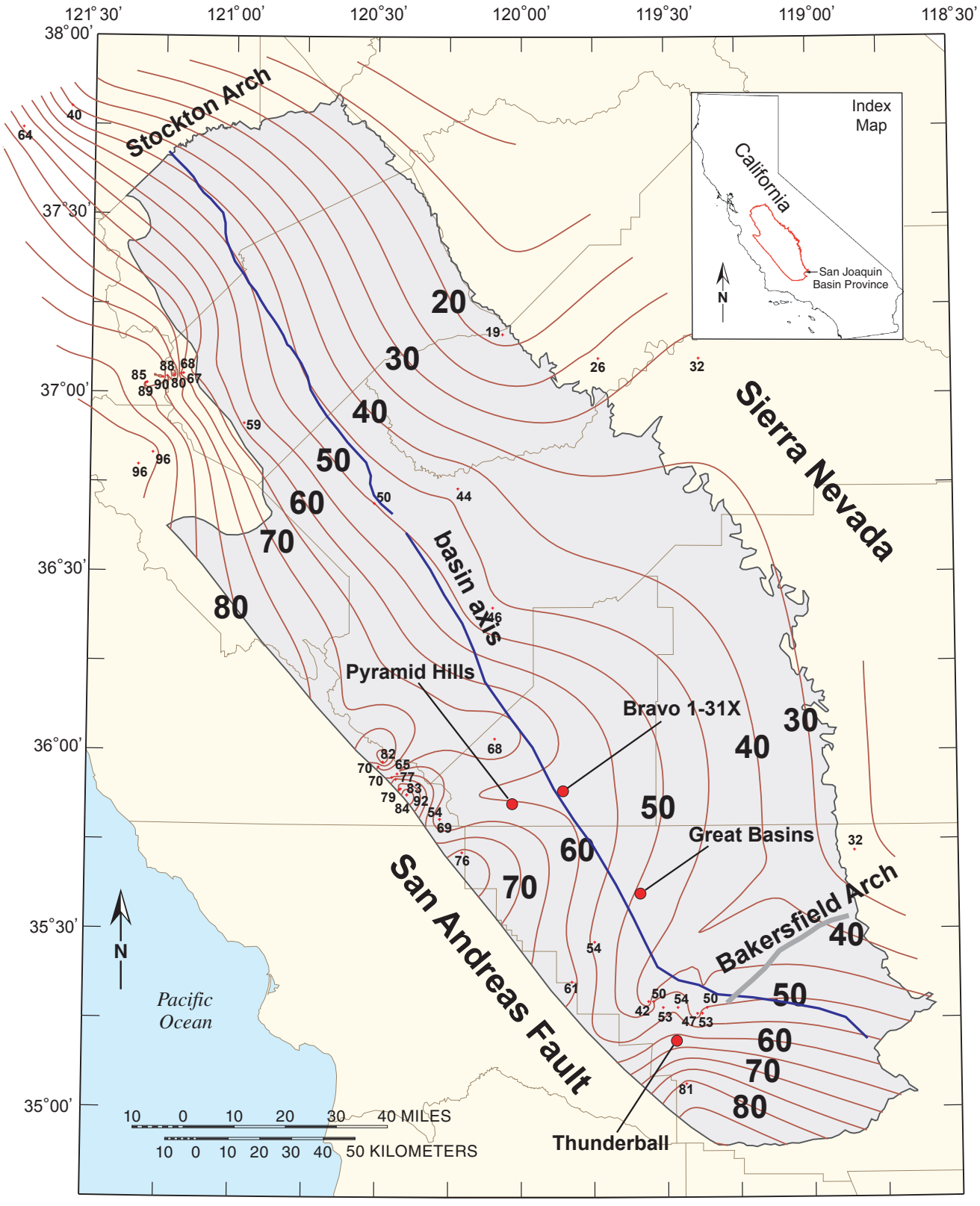

Figure 12.7. Present-day surface heat flow based on gridded and contoured data from 42 shallow core holes in and around the San Joaquin Basin study area (data courtesy of Colin Williams, USGS, 2004). Each core hole (red-cross symbol) is labeled with the corresponding observed heat-flow value in units of milliwatts per square meter (mW/m^2). Contour interval is 5 mW/m^2; contours values are plotted in bold type. County boundaries are plotted as thin brown lines. San Joaquin Basin Province boundary is shown in gray. Basin axis and Bakersfield Arch are as in figure 12.1. The four calibration wells (filled red circles) are discussed in the text and figure 12.8.

heat flow. Initial versions of the 4-D model used standard PetroMod® "basement" lithology and associated thermal and physical properties throughout the study area. However, calibrations of wells were not satisfactory using this approach because of insufficient basal heat flow to the east of the basin axis. We found that use of standard PetroMod® "basement" to the west and more radioactive PetroMod® "granite" lithology to the east of the basin axis gave the most satisfactory

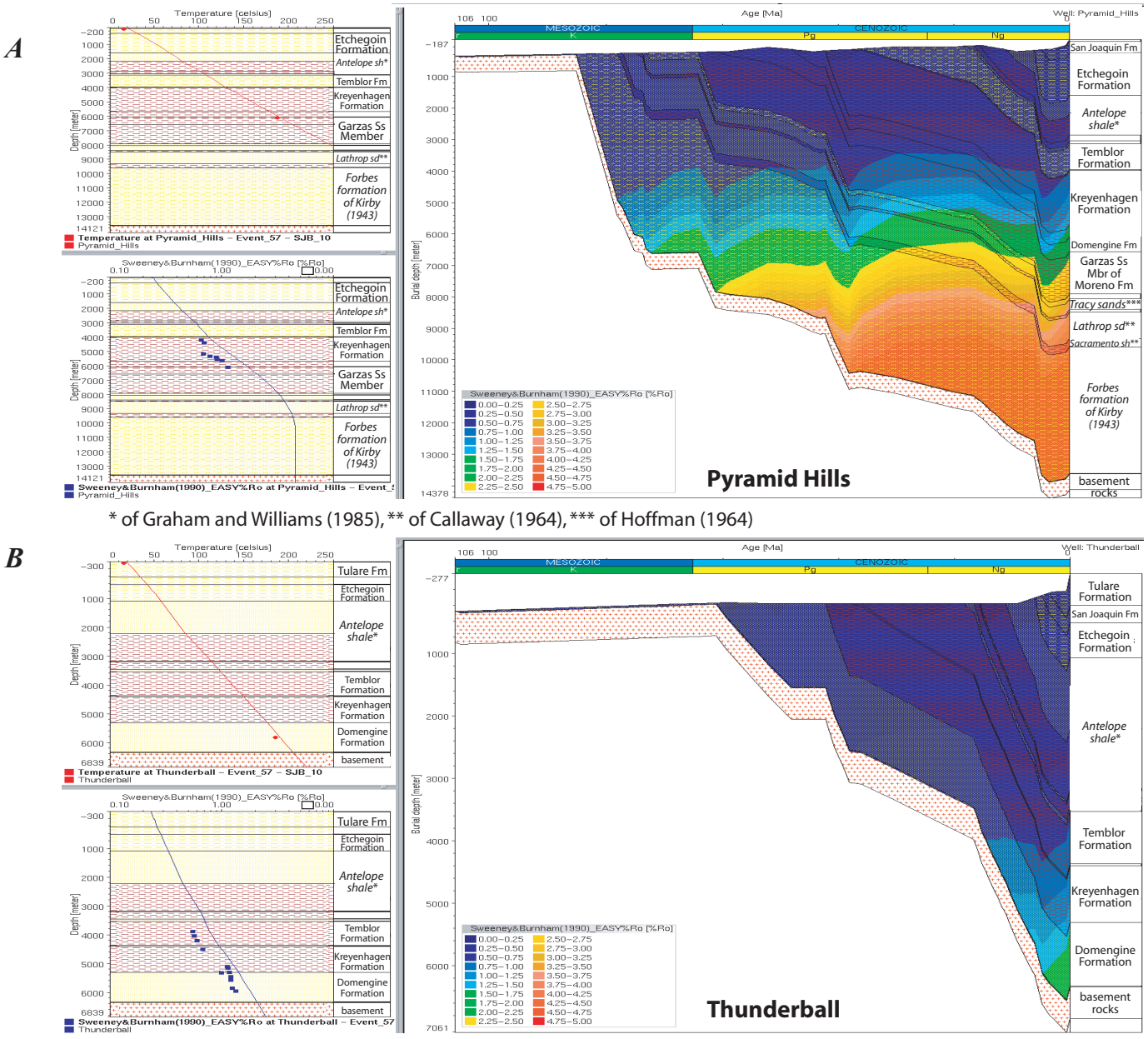

Figure 12.8. Four one-dimensional (1-D) extractions from the four-dimensional (4-D) petroleum systems model at *A*, Pyramid Hills 1-9; *B*, Thunderball 954-35B; *C*, Great Basins 31X-10; and *D*, Bravo 1-31X wells in the San Joaquin Basin. Each of the four extractions includes three data sets. The inset at upper left shows measured surface and equilibrated bottom-hole temperatures (data shown by red-diamond symbols) compared to the temperature calculated by the 4-D model (red curve). The inset at lower left shows vitrinite reflectance values (data shown by blue square symbols) compared to calculated vitrinite reflectance (blue curve). The large inset at right shows vitrinite reflectance calculated by the 4-D model for each rock unit through time. Reflectance data for the Bravo 1-31X well are from the nearby Pyramid Hills-1 and Chevron 73-30 wells. These calibrations used PetroMod® standard "basement" and more radioactive "granite" lithologies and associated thermal and physical properties for basement composition to the west (Pyramid Hills and Thunderball) and east (Great Basins and Bravo) of the basin axis (fig. 12.1), respectively. See figure 12.7 for well locations. Formation names in italics are informal. Well names Pyramid Hills 1-9, Thunderball 954-35B, Bravo 1-31X, and Great Basins 31X-10 are formally described by their American Petroleum Institute numbers (04031204230000, 04030186880000, 04031201350000, and 04029473610000, respectively). Positive and negative depth values indicate depth below or elevation above sea level, respectively. Fm, Formation; Mbr, Member; sd, sand; Ss, Sandstone; sh, shale.

calibrations for all wells. The resulting basal heat flow yields predicted thermal maturities and volumes of petroleum that are reasonably similar to observations in the basin, as discussed below.

The Pyramid Hills 1-9, Thunderball 954-35B, Bravo 1-31X, and Great Basins 31X-10 wells are four examples of wells used in this study for heat flow calibration (fig. 12.8). Detailed stratigraphy from well logs was available for all four wells. For the Pyramid Hills and Thunderball wells, we used vitrinite reflectance and equilibrated bottom-hole temperatures determined in those wells. For the Bravo well, which lacked useful vitrinite reflectance and bottom-hole temperature data, we used data from the nearby Pyramid Hills-1 and Chevron 73-30 wells. The Great Basins 31X-10 well was calibrated using vitrinite reflectance and bottom-hole temperature data from the nearby East Lost Hills 9-2 well.

Tmax data from Rock-Eval pyrolysis (Peters and Cassa, 1994) were available in many wells having vitrinite reflectance data. We checked the quality of the measured vitrinite reflectance data used for calibration by comparing it to vitrinite reflectance (percent) calculated from Tmax (°C) using the following formula:

C

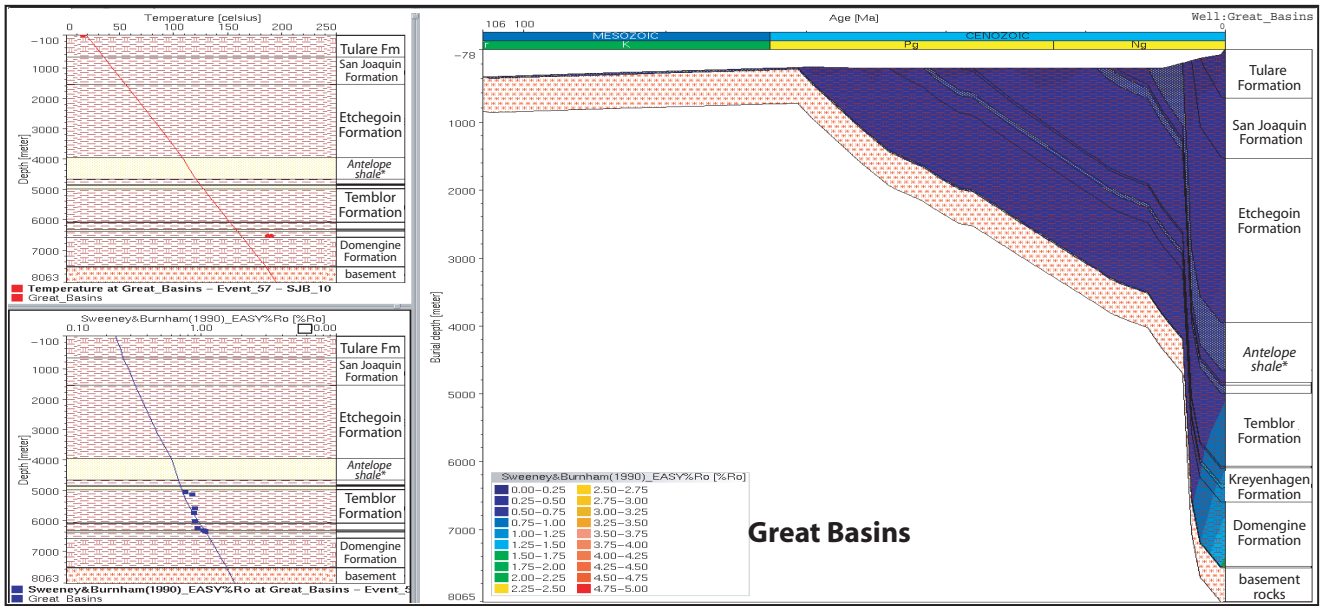

* of Graham and Williams (1985)

D

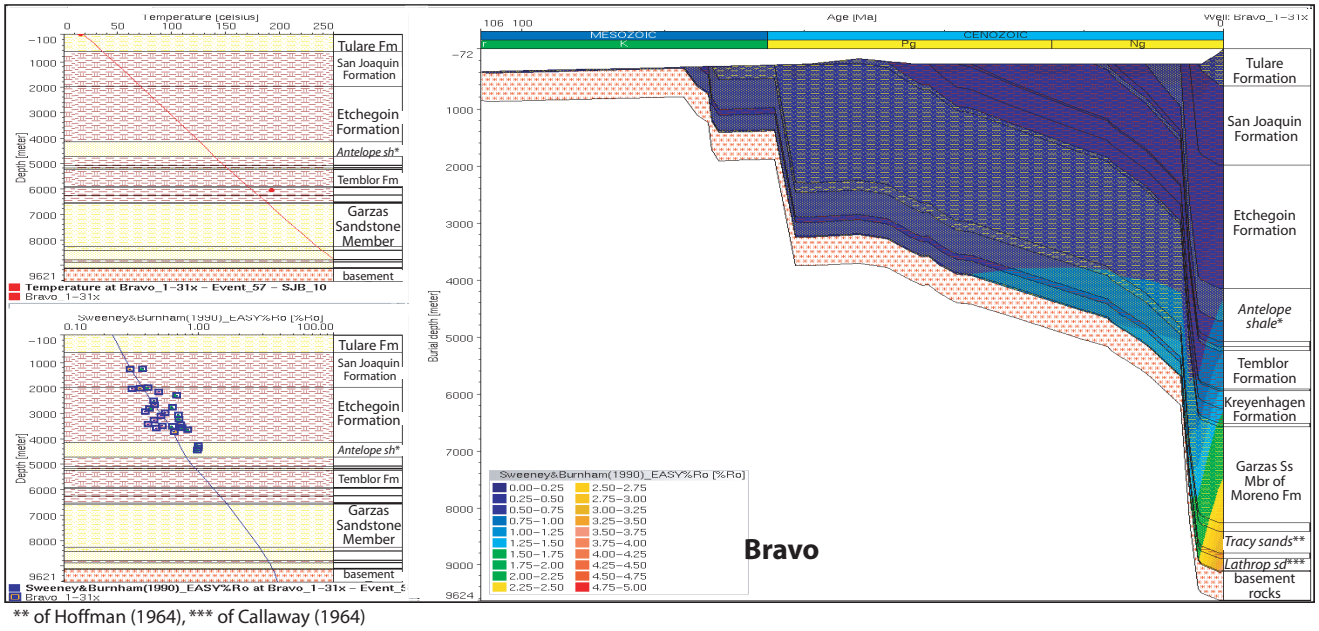

** of Hoffman (1964), *** of Callaway (1964)

Figure 12.8.—Continued.

Vitrinite reflectance (calculated) = (0.0180)(Tmax) – 7.16

This formula is based on data for a collection of shales containing low-sulfur Type II or Type III kerogen (Jarvie and others, 2001). It is not applicable for Type I kerogen. The curve generated by the formula corresponds reasonably well with empirical observations of Tmax versus vitrinite reflectance for Type III kerogens (Teichmüller and Durand, 1983). Use of the formula is not recommended for very low or very high maturity samples (where Tmax is less than 420°C or greater than 500°C) or when S2 is less than 0.5 mg hydrocarbon/g rock. "Caving" of rock cuttings from shallow to deeper parts of the wellbore during drilling can invalidate these calculations because the caved material represents a contaminant that is less thermally mature than the deeper rock cuttings. Because of inaccuracies related to measurements of Tmax on single samples, it is best to interpret a Tmax trend to establish equivalent vitrinite reflectance values.

4-D Model Output

Typical output for each depositional or erosional event in the petroleum systems model includes rock unit thickness after compaction, porosity, pressure, temperature, and thermal maturity at depth, generated volume of petroleum, expulsion efficiency, migration pathways, and accumulated volume of petroleum.

Discussion

Modeled Thermal Maturity

Antelope shale

Petroleum systems are described using the source-rock name followed by a hyphen, the principal reservoir formation name, and an indication of the certainty of the correlation. The symbols (?), (.), and (!) indicate speculative, hypothetical, and known genetic relationships, respectively (Magoon and Dow, 1994). The combined Antelope-Stevens(!) and McLure-Tulare(!) petroleum systems (south and north of the Bakersfield Arch, respectively) account for about 12.2 billion barrels of oil (BBO) and 13.1 trillion cubic feet of gas (TCFG) making them the two largest petroleum systems in the San Joaquin Basin (Magoon and others, this volume, chapter 8).

The 4-D PetroMod® model confirms that burial depths of 4.0 to 4.6 km (13,000 to 15,000 ft) are required for oil generation from the Antelope shale source rock (Graham and Williams, 1985; Kruge, 1986). Although the proper designation for the Miocene source rock north of the Bakersfield Arch is McLure Shale (a member of the Monterey Formation), we use the term "Antelope shale" to simplify the following discussion. The 4-D model predicts that the Antelope shale is thermally immature, except in two areas designated as the Tejon and Buttonwillow depocenters (fig. 12.9). Within these depocenters the source rock is buried deepest in three areas that we describe as the "Northern Buttonwillow," "Southern Buttonwillow," and "Tejon" (also called Maricopa) depocenters (fig. 12.9). The base of the Antelope shale in these depocenters has present-day predicted vitrinite reflectance values and transformation ratios greater than 1 percent and greater than 50 percent, respectively. Maximum vitrinite reflectance and transformation ratios in the Northern Buttonwillow and Tejon depocenters surpass 1.5 percent and 85 percent, respectively, but are significantly less in the Southern Buttonwillow depocenter (about 1.0 percent and 55 percent, respectively).

The Tejon depocenter is highly favorable for petroleum generation from the Antelope shale source rock compared to the Northern and Southern Buttonwillow depocenters. At depths greater than about 3.7 km (12,000 ft) in this depocenter, the source rock is 900 to 1,200 m (3,000 to 4,000 ft) thick and contains "very good to excellent" quantities of original total organic carbon (2.0 to 5.5 weight percent) consisting mainly of oil-prone type II or type IIS organic matter prior to thermal maturation (original hydrogen indices in the range 300 to 400 mg hydrocarbon/g total organic carbon; Peters, Magoon, Valin, and Lillis, this volume, chapter 11; table 12.2). (Terms to describe the amount and quality of organic matter in source rocks are defined by Peters and Cassa, 1994.) The Southern Buttonwillow depocenter contains Antelope shale having organic richness similar to that in the Tejon depocenter, but it is thinner (table 12.2), less thermally mature, and covers a smaller area than that in the Tejon depocenter (fig. 12.9). The Northern Buttonwillow depocenter contains Antelope shale with thermal maturity similar to that in the Tejon depocenter, but it has comparatively low original total organic carbon and hydrogen index values (table 12.2). For example, Antelope shale in the Northern Buttonwillow depocenter had only 1 to 2 weight percent original total organic carbon and 200 to 350 mg hydrocarbon/g total organic carbon (Peters, Magoon, Valin, and Lillis, this volume, chapter 11). Calculations suggest that regardless of original hydrogen index, expulsion efficiencies for rocks containing less than 1 to 2 weight percent original total organic carbon will be low (Peters and others, 2005). This is consistent with petrographic observations of Late Devonian to Early Mississippian Woodford Shale from Oklahoma and related units, which suggest that rocks with less than 2.5 weight percent original total organic carbon may be incapable of establishing the continuous bitumen network required for primary migration and expulsion of crude oil (Lewan, 1987)

Tumey formation

The Tumey-Temblor(.) petroleum system accounts for 0.6 BBO and 2.1 TCFG in the San Joaquin Basin (Magoon and others, this volume, chapter 8). Unlike the other petroleum systems in this study, the Tumey-Temblor(.) petroleum system is hypothetical because no definitive geochemical correlations

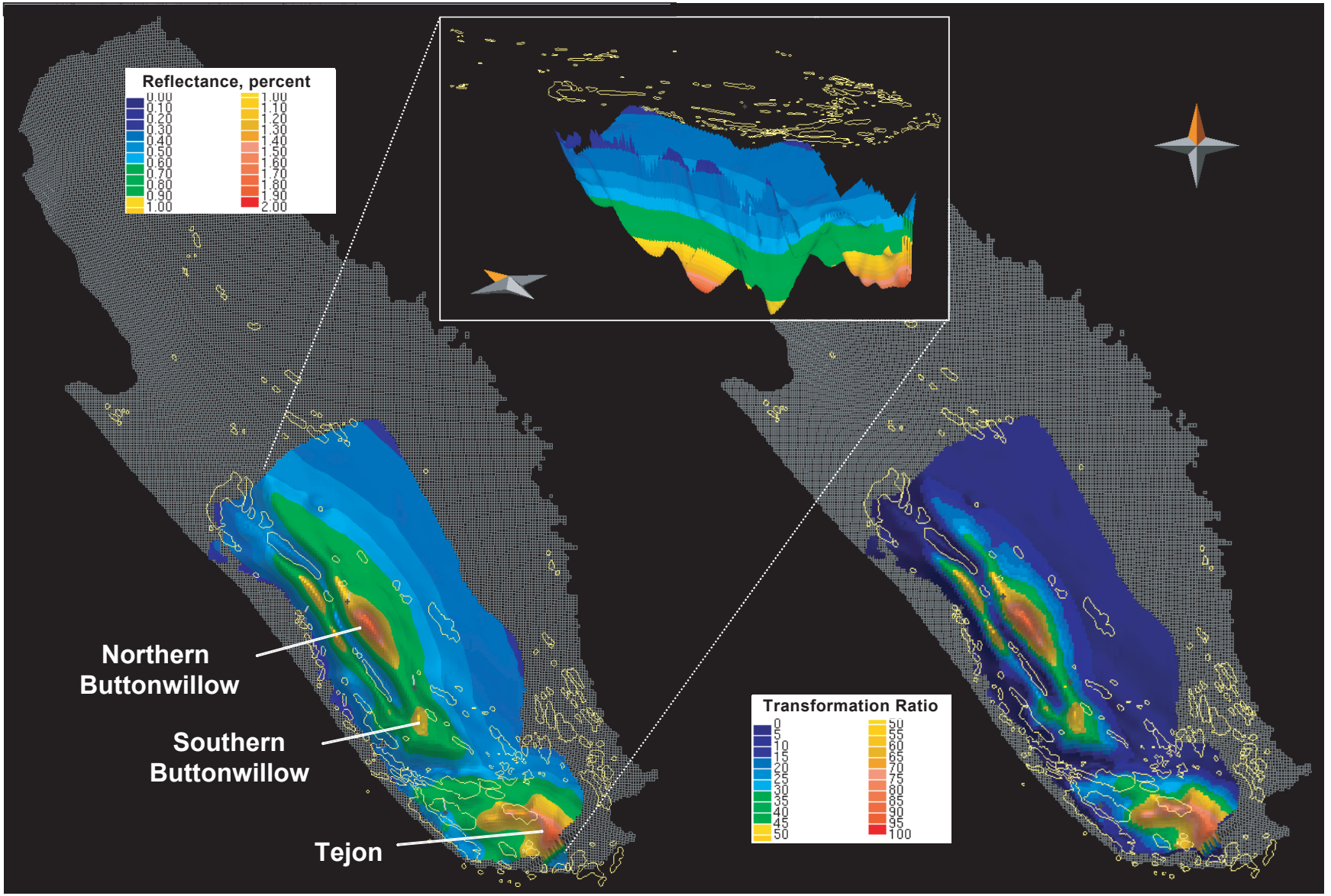

Figure 12.9. Map of calculated present-day thermal maturity expressed as vitrinite reflectance (percent, left) and transformation ratio (percent; right) for the Antelope shale source rock. Vitrinite reflectance was calculated using the "Easy%R_o" method of Sweeney and Burnham (1990). Inset shows an inclined, northeastward view of predicted Antelope shale thermal maturity, which is greatest at the base of the unit in each depocenter. Vertical one-dimensional (1-D) extractions were completed in the deepest portions of the Tejon (fig. 12.12), Southern Buttonwillow (fig. 12.13), and Northern Buttonwillow (fig. 12.14) depocenters.

Table 12.2. Comparison of thickness, original total organic carbon (TOCo), and original hydrogen index (HIo) with timing of initial, peak, and the end of oil expulsion for the Antelope shale, Kreyenhagen Formation, and Moreno Formation source rocks in depocenters or generative areas in the San Joaquin Basin. TR is the transformation ratio, which is the difference between the original hydrocarbon potential of a rock prior to maturation and the measured hydrocarbon potential, divided by the original hydrocarbon potential.

Source Rock	Depocenter or Area	Thickness, ft (m)	TOC_o, weight percent†	HI_o, mg hydrocarbon/g total organic carbon	Initial Expulsion (10 percent TR), Ma††	Peak Expulsion (50 percent TR), Ma††	End Expulsion (95 percent TR), Ma*
Antelope shale-McLure Shale	Tejon	3,000-4,000 (914-1,219)	2.0-5.5 [3.5-5.5]	300-400	4.6	3.6	(86 percent)
	Southern Buttonwillow	500-1,000 (152-305)	3.5-4.5	300-400	4.2	0.5-1.0	(52 to 56 percent)
	Northern Buttonwillow	500-1,000 (152-305)	1.0-2.0	200-350	4.7	3.2-3.5	(83 to 87 percent)
Kreyenhagen Formation	Tejon**	0-400 (0-122)	1.0-2.0	100-250	[4.7]	[4.1]	[3.1]
	Southern Buttonwillow	400-800 (122-244)	2.0-3.0	150-250	4.2	2.5	(95 percent)
	Northern Buttonwillow	400-800 (122-244)	2.0-3.0	350-450	5.5	4.3	3.6
Moreno Formation	Jacalitos field area	500-700 (152-213)	3.5-4.0	300-350	58	54	46

†Total organic carbon for Antelope shale in the Tejon depocenter may require revision to higher values (in brackets) because the sampled intervals in three control wells only penetrate the upper few hundred meters of source rock and may not be representative of deeper Antelope shale. The bracketed values are the result of interpolation of data remaining after exclusion of the data from these three wells (see Peters, Magoon, Valin, and Lillis, this volume, chapter 11).

††Initial expulsion occurs at 5 percent saturation in PetroMod®, which we equated with 10 percent transformation ratio. Ranges of values are ages of peak expulsion for the top and bottom of the unit. If no range is given, the top and bottom differ by no more than about 0.1 Ma.

*Values in parentheses are present-day transformation ratios (source-rock unit has not yet reached end of oil expulsion at transformation ratio of 95 percent). Ranges of values are transformation ratios for the top and bottom of the unit. If no range is given, the top and bottom differ by no more than about 1 percent transformation ratio.

**Kreyenhagen Formation is absent, except in the northernmost part of the Tejon depocenter. Calculated times of initial, peak, and end expulsion in brackets assume that some Kreyenhagen Formation exists in the deepest part of the Tejon depocenter.

have been published. However, some geochemical and geologic evidence suggests that a genetic oil-source rock correlation exists. For example, the Deer Creek oil field on the east flank of the basin is thought to contain oil from the Tumey formation source rock (Lillis and Magoon, this volume, chapter 9).

Most of the petroleum expelled from the Tumey formation accumulated in the overlying Temblor Formation reservoir facies, but it accounts for less than 0.5 percent of accumulated oil in the 4-D model. For this reason and because it is difficult to differentiate petroleum generated by Tumey shale versus that generated within the Kreyenhagen Formation, the discussion focuses on the immediately underlying and far more prolific Kreyenhagen Formation.

Kreyenhagen Formation

The Kreyenhagen-Temblor(!) petroleum system accounts for about 1.8 BBO and 3.0 TCFG in the province (Magoon and others, this volume, chapter 8). Burial depths of about 4.6 km (15,000 ft) are needed to generate oil from the Kreyenhagen Formation source rock according to our 4-D petroleum systems model. Kreyenhagen Formation source rock is thin or absent in the Tejon depocenter. However, organic-rich shale of the Kreyenhagen Formation in the Buttonwillow depocenters underwent extensive thermal maturation (fig. 12.10). The model predicts that Kreyenhagen Formation source rock has present-day vitrinite reflectance values and transformation ratios of more than 1.3 percent and about 95 percent, respectively, in the Southern Buttonwillow depocenter and more than 2.0 percent and 100 percent, respectively, in the Northern Buttonwillow depocenter. Most of the petroleum expelled from the Kreyenhagen Formation in both the model and nature accumulated in the overlying Temblor Formation and Etchegoin Formation reservoir facies.

Moreno Formation

Burial depth of about 4.6 km (15,000 ft) is required to generate oil from the Moreno Formation source rock according to our 4-D petroleum systems model (fig. 12.11). Organic-

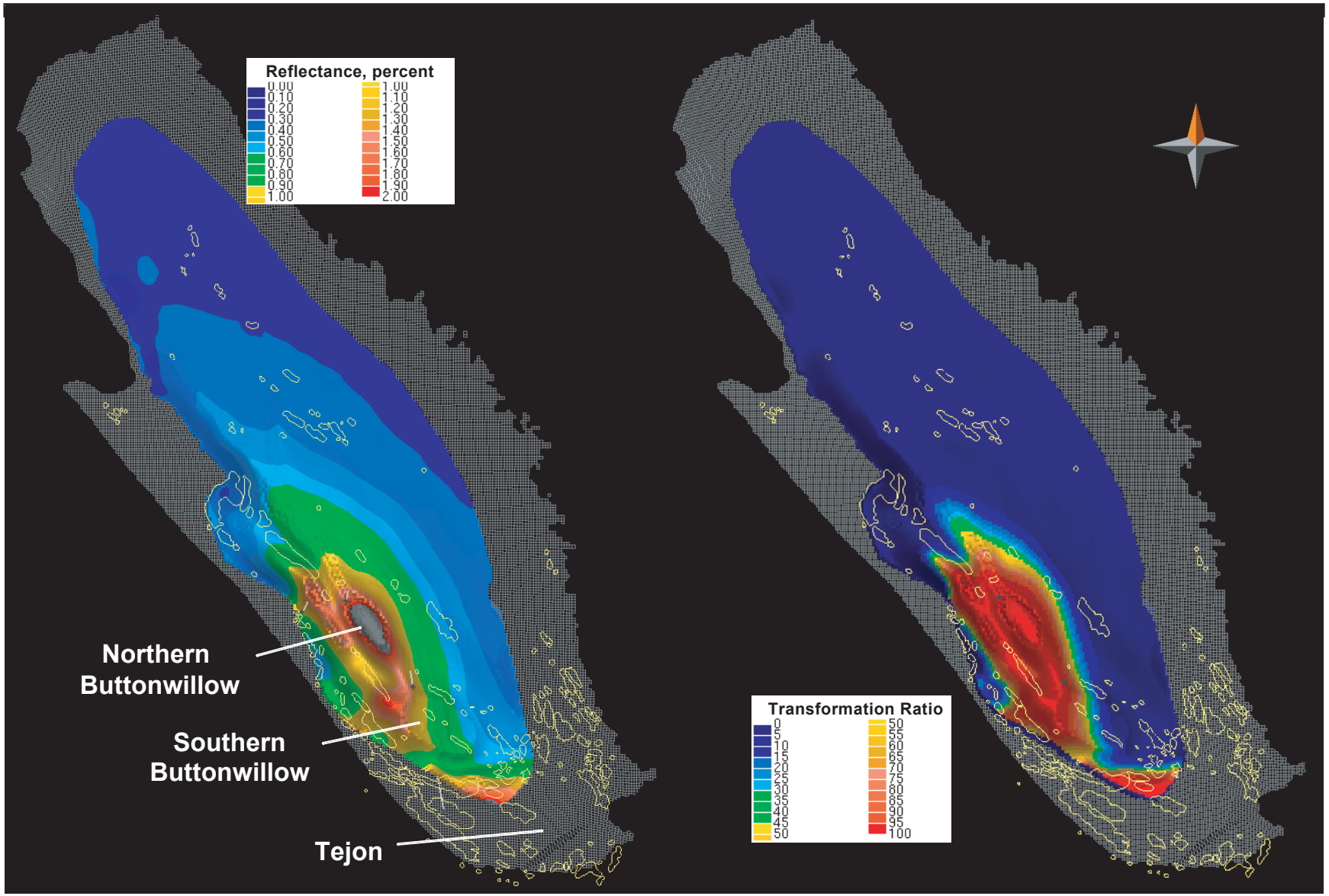

Figure 12.10. Map of calculated present-day thermal maturity expressed as vitrinite reflectance (percent, left) and transformation ratio (percent, right) for the Kreyenhagen Formation source rock. Vitrinite reflectance was calculated using the "Easy%R_o" method of Sweeney and Burnham (1990). The gray area in the center of the Northern Buttonwillow depocenter (left) indicates vitrinite reflectance for Kreyenhagen Formation greater than 2.0 percent.

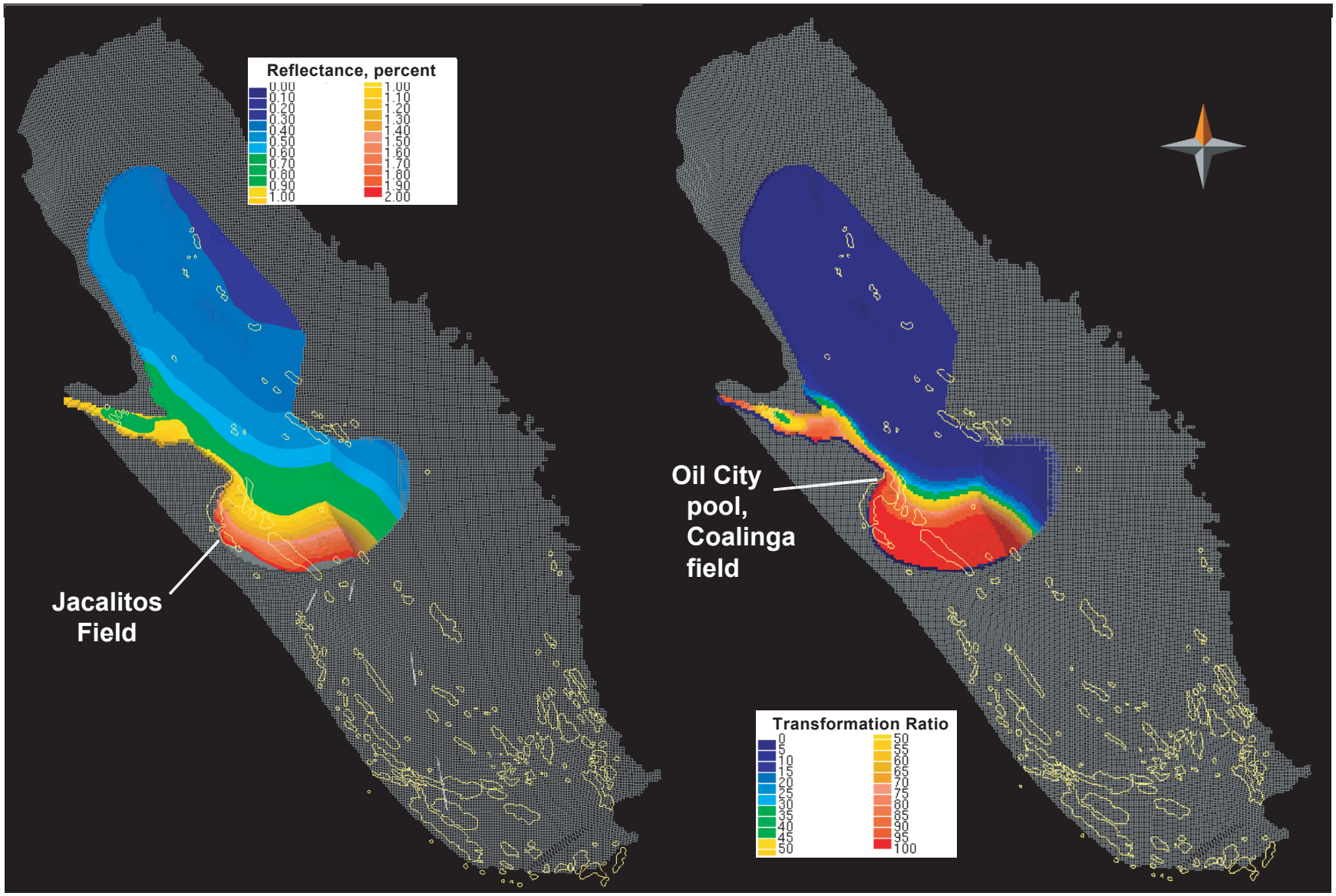

Figure 12.11. Map of calculated present-day thermal maturity expressed as vitrinite reflectance (percent, left) and transformation ratio (percent, right) for the Moreno Formation source rock. Vitrinite reflectance was calculated using the "Easy%R_o" method of Sweeney and Burnham (1990). A one-dimensional (1-D) extraction (fig. 12.15) was obtained immediately southeast of the Jacalitos field, which is in the area where vitrinite reflectance exceeds 2.0 percent (shown in gray) near the erosional edge of the Moreno Formation.

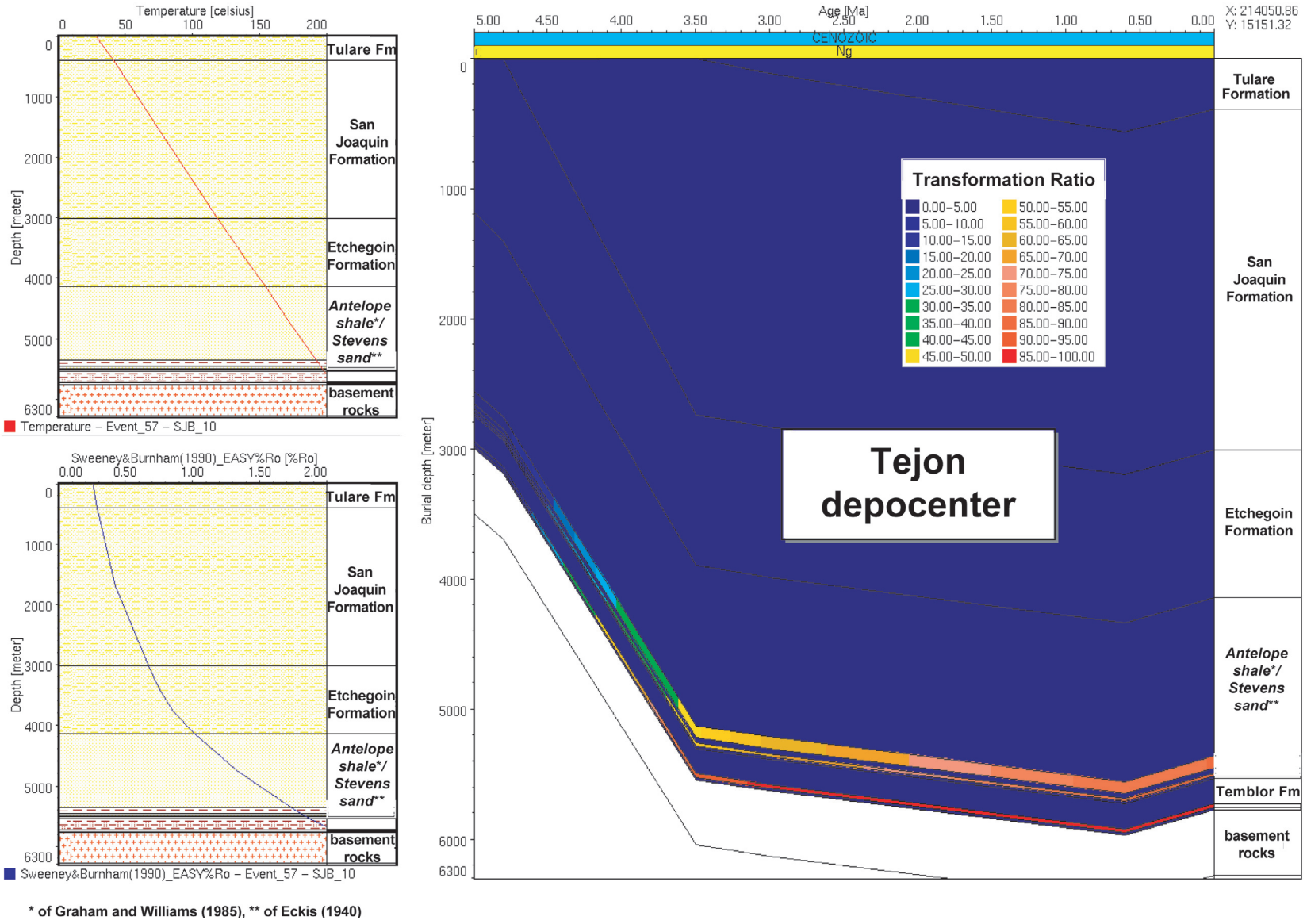

Figure 12.12. One-dimensional (1-D) burial-history model extracted from the deepest portion of the Tejon depocenter shows calculated temperature (top left), vitrinite reflectance (bottom left), and transformation ratio (percent, right) for the Antelope shale and Kreyenhagen Formation source rocks. On the basis of the transformation ratio plot, the Antelope shale source rock began to expel petroleum (10-percent transformation ratio) about 4.6 Ma and reached peak expulsion (50-percent transformation ratio) about 3.6 Ma (table 12.2). This source rock has reached 86 percent transformation ratio at this location, and thus has not yet reached the end of oil expulsion (95-percent transformation ratio). The Kreyenhagen Formation source rock is thin or absent in the Tejon depocenter. If present, the model predicts that Kreyenhagen Formation began to expel petroleum about 4.7 Ma, reached peak expulsion about 4.1 Ma, and reached the end of oil expulsion about 3.1 Ma at this location. Formation names in italics are informal. Fm, Formation.

rich Moreno Formation source rock near the Jacalitos field (about 3 weight percent total organic carbon) underwent severe thermal maturation, resulting in present-day vitrinite reflectance values and transformation ratios in the range of about 2.0 to 2.5 percent and about 100 percent, respectively. The 4-D model confirms that petroleum generated from the Moreno Formation source rock is dominated by hydrocarbon gas and light oil trapped within the same formation. The Moreno-Nortonville gas system probably accounts for only about 158 thousand barrels of oil and about 183 billion cubic feet of hydrocarbon gas (BCFG), mostly in the small Oil City pool of Coalinga field (Magoon and others, this volume, chapter 8).

Although geological and geochemical evidence suggests that the Moreno Formation source rock accounts for the Oil City accumulation (fig. 12.11; Peters and others, 1994), an attempt to correlate the oil with pyrolyzed Moreno Formation (Marca Shale Member) source rock was unconvincing (Fonseca-Rivera, 1998). Interestingly, the only significant accumulation of light oil generated from the Moreno Formation by the 4-D petroleum systems model occurs in the vicinity of the Oil City pool. The 4-D model thus supports interpretations that oil in the Oil City pool of Coalinga field originated from Moreno Formation source rock near the Jacalitos field area and migrated stratigraphically updip within the Moreno Formation and overlying Domengine Formation (Lillis and Magoon, this volume, chapter 9; Peters and others, 1994).

Expulsion Timing

The timing of initial, peak, and end of oil expulsion (depletion of oil potential) from the source rock are important factors that help to determine the maximum volumes of petroleum that might accumulate in traps. For purposes of discussion, we have chosen the beginning, peak oil, and end of oil expulsion to correspond to transformation ratios of 10 percent, 50 percent, and 95 percent, respectively (table 12.2). Gas generation from kerogen begins and ends at transformation ratios of 10 percent and 95 percent, respectively, and oil cracking to gas begins at transformation ratios of 10 percent.

Thick, organic-rich potential source rocks cannot become effective source rocks without sufficient burial and thermal maturation. Because the effective source rocks in the San Joaquin Basin are now at or near their maximum burial depth, comparison of thickness and organic richness information for these rocks can be simplified by focusing on the various depocenters. The following discussion describes the timing of initial, peak, and end of oil expulsion within the three key depocenters and one additional generative area in the San Joaquin Basin study area.

Tejon Depocenter

On the basis of a 1-D burial history model or "pseudo-well" extracted from the 4-D model in the deepest portion of the Tejon depocenter (table 12.2; fig. 12.12), the Antelope shale source rock began to expel petroleum about 4.6 Ma and reached peak expulsion about 3.6 Ma. The difference in timing of petroleum expulsion between the bottom and top of the Antelope shale source rock at this locality is small (less than 0.1 Ma). The model predicts that the Antelope shale in the deepest portion of the Tejon depocenter is thermally mature (transformation ratio about 86 percent), but has not reached the end of oil expulsion (defined as 95 percent transformation ratio; fig. 12.12). Generation and expulsion of petroleum from this source rock continue today throughout the Tejon depocenter.

Kreyenhagen Formation source rock is thin or absent in the Tejon depocenter (fig. 12.10). If we assume that a thin shale interval of the Kreyenhagen Formation occurs in the deepest portion of the depocenter, the extracted 1-D burial history at that location predicts that expulsion from Kreyenhagen Formation source rock began about 4.7 Ma, and that peak expulsion and end of oil expulsion were reached about 4.1 and 3.1 Ma, respectively (table 12.2; fig. 12.12). Thus, any Kreyenhagen Formation in the deepest portions of the Tejon depocenter can no longer generate oil, although small amounts of gas might still be generated.

Southern Buttonwillow Depocenter

The 1-D burial history model extracted from the deepest portion of the Southern Buttonwillow depocenter (table 12.2; fig. 12.13) predicts that the Antelope shale source rock began to expel petroleum about 4.2 Ma and reached peak expulsion about 0.5 to 1.0 Ma. The Antelope shale in this depocenter has achieved a transformation ratio of about 52 to 56 percent and thus is still generating significant volumes of oil even in the deepest areas.

Shale of the Kreyenhagen Formation in the Southern Buttonwillow depocenter began expulsion about 4.2 Ma and reached peak expulsion about 2.5 Ma. The shallower Antelope shale began expulsion about the same time as the Kreyenhagen Formation because the kinetics for kerogen in the Antelope shale (Type IIS) results in faster petroleum generation than those for the Kreyenhagen Formation (Type II). The present-day transformation ratio of Kreyenhagen Formation in the deepest portion of the depocenter is about 95 percent, indicating that the source rock has little or no remaining petroleum generative potential. However, oil expulsion is still proceeding within the Kreyenhagen Formation at shallower depths in this depocenter.

Northern Buttonwillow Depocenter

The 1-D burial history model extracted from the deepest portion of the Northern Buttonwillow depocenter (table 12.2; fig. 12.14) indicates generally higher thermal maturity than

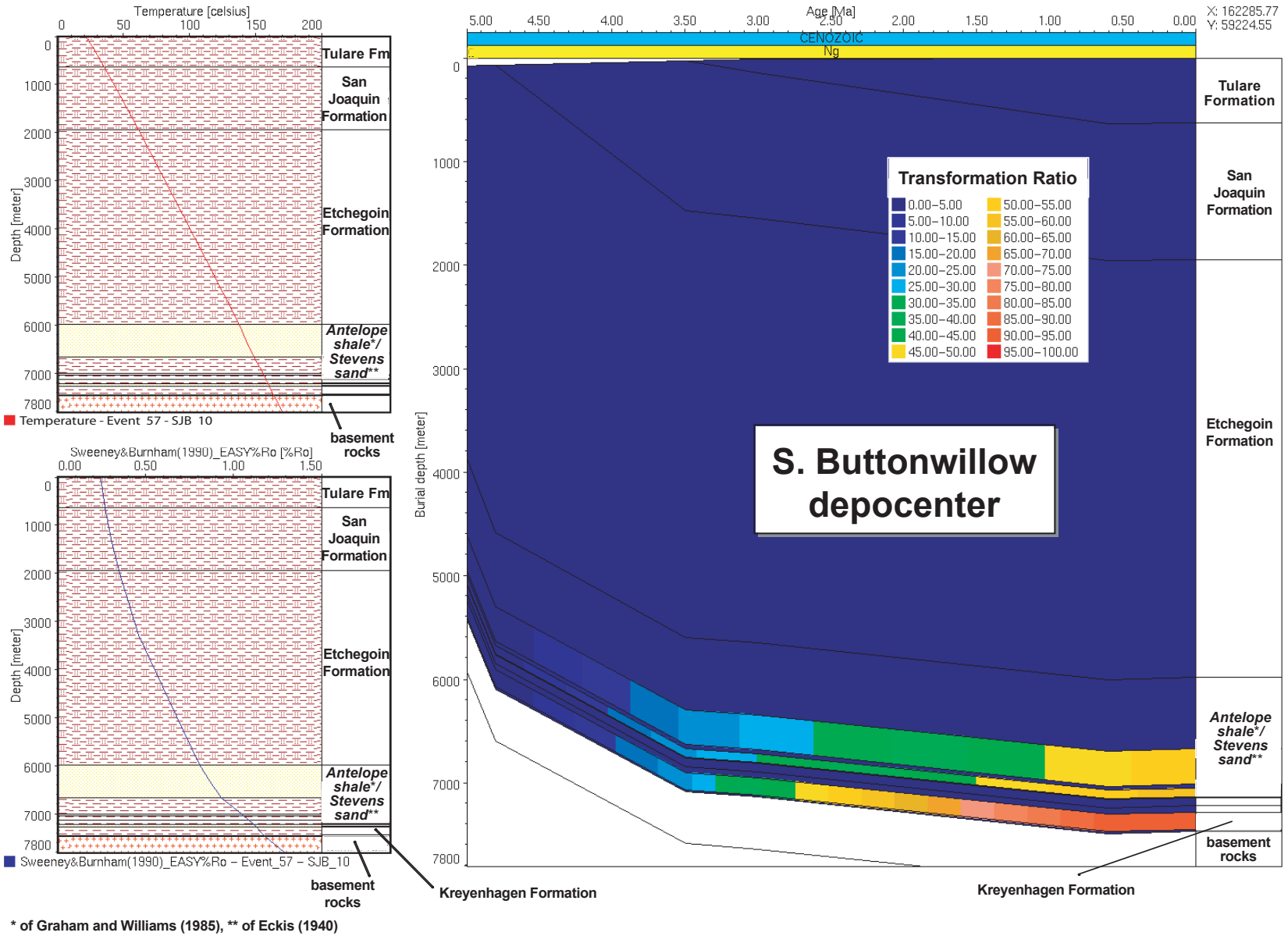

* of Graham and Williams (1985), ** of Eckis (1940)

Figure 12.13. One-dimensional (1-D) burial-history model extracted from the deepest portion of the Southern Buttonwillow depocenter shows calculated temperature (top left), vitrinite reflectance (bottom left), and transformation ratio (percent, right) for the Antelope shale and Kreyenhagen Formation source rocks. On the basis of the transformation ratio plot, the Antelope shale source rock began to expel petroleum (10-percent transformation ratio) about 4.2 Ma and reached peak expulsion (50-percent transformation ratio) in the range 0.5 to 1.0 Ma (top versus bottom of unit; table 12.2). The Antelope shale at this location has transformation ratios of 52 to 56 percent and thus has not yet reached the end of oil expulsion (95-percent transformation ratio). The Kreyenhagen Formation source rock began to expel petroleum about 4.2 Ma, reached peak expulsion about 2.5 Ma, and has reached 95-percent transformation ratio at this location. Formation names in italics are informal. Fm, Formation.

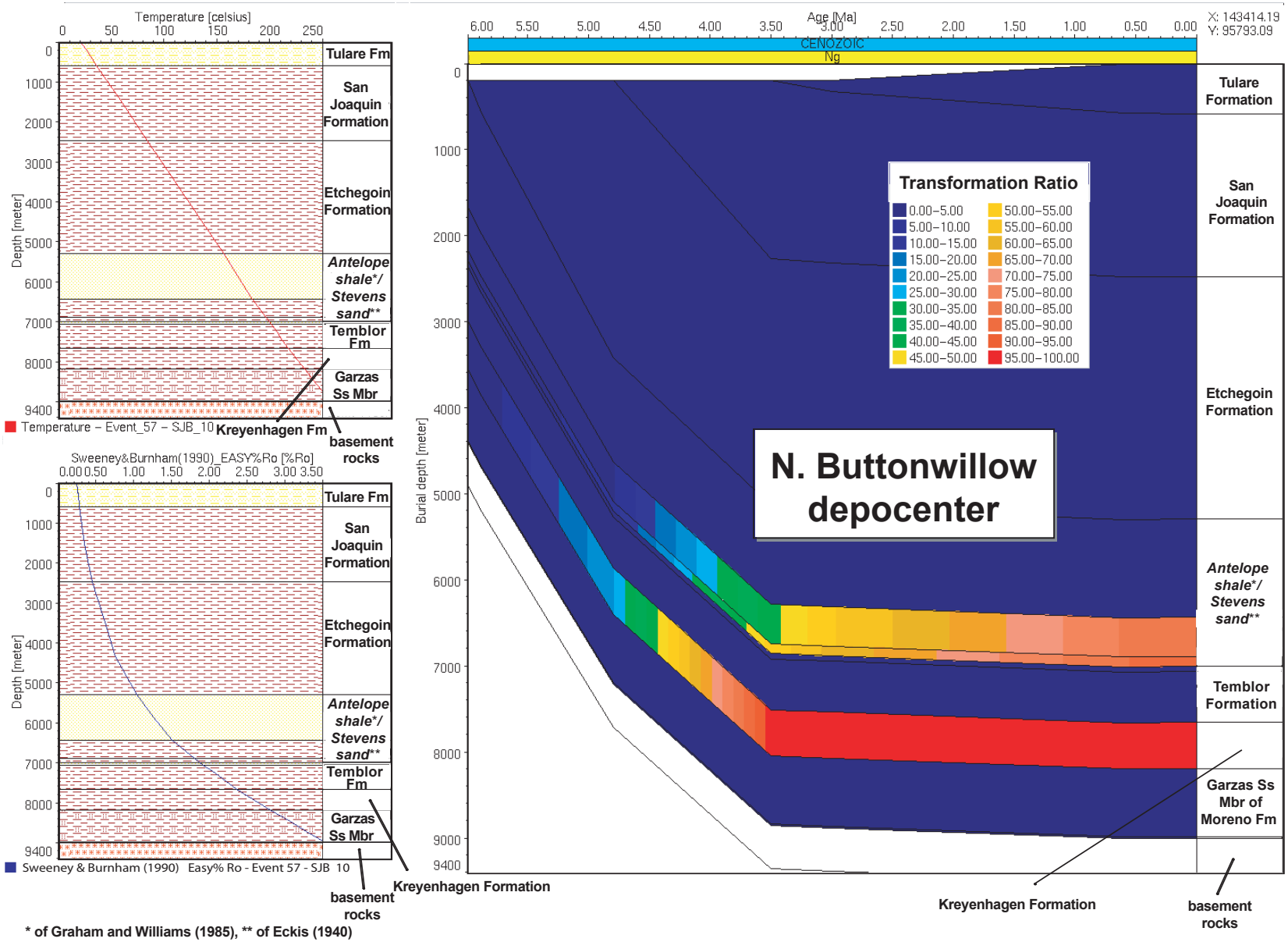

Figure 12.14. One-dimensional (1-D) burial-history model extracted from the deepest portion of the Northern Buttonwillow depocenter shows calculated temperature (top left), vitrinite reflectance (bottom left), and transformation ratio (percent, right) for the Antelope shale and Kreyenhagen Formation source rocks. On the basis of the transformation ratio plot, the Antelope shale source rock began to expel petroleum (10-percent transformation ratio) about 4.7 Ma and reached peak expulsion (50-percent transformation ratio) in the range 3.2 to 3.5 Ma (top versus bottom; table 12.2). This Antelope shale has reached 83 to 87 percent transformation ratio at this location, and thus has not yet reached the end of oil expulsion (95-percent transformation ratio). The Kreyenhagen Formation began to expel petroleum about 5.5 Ma, reached peak expulsion about 4.3 Ma, and reached the end of oil expulsion about 3.6 Ma at this location. Formation names in italics are informal. Fm, Formation; Mbr, Member; Ss, Sandstone.

in the Southern Buttonwillow depocenter. The model predicts that the Antelope shale source rock began expulsion about 4.7 Ma and reached peak expulsion about 3.2 to 3.5 Ma. Antelope shale in the deepest portion of the depocenter has achieved a transformation ratio of 83 to 87 percent.

The model predicts that the Kreyenhagen Formation in the Northern Buttonwillow depocenter began expulsion about 5.5 Ma and reached peak expulsion about 4.3 Ma. The Kreyenhagen Formation reached the end of oil expulsion about 3.6 Ma in this depocenter.

Jacalitos Field Area

Moreno Formation source rock in the area immediately southeast of the Jacalitos field now exhibits high thermal maturity. The 1-D burial history model extracted from the most thermally mature part of the Jacalitos field area (table 12.2; fig. 12.15) indicates that the Moreno Formation source rock began to expel petroleum about 58 Ma, reached peak expulsion about 54 Ma, and reached the end of oil expulsion about 46 Ma.

Predicted Locations and Volumes of Accumulations

On the basis of discovered oil fields, a large volume of recoverable oil (about 12.2 BBO) and associated gas (about 13.1 TCFG) in the San Joaquin Basin migrated and accumulated in reservoir rocks from Antelope shale source rock that still has petroleum generative potential. The 4-D petroleum systems model fails to trap as much oil as occurs in known fields (Magoon and others, this volume, chapter 8). The current model traps a total oil volume of about 16 BBO, of which only 48 percent is oil generated by Antelope shale (about 8 BBO) and only a portion is recoverable. The amount of trapped oil from the Antelope shale source rock might be increased in a subsequent model, for example, by revising the mapped original total organic carbon content near the Tejon depocenter (table 12.2; see also fig. 11.11 in Peters, Magoon, Valin, and Lillis, this volume, chapter 11).

To acquire a qualitative view of when most petroleum was expelled from each source rock and became available for entrapment, we calculated oil volumes generated per unit of rock mass at various geologic times (figs. 12.16 through 12.18). For example, the 4-D model predicts that although peak expulsion from the Antelope shale source rock occurred as early as 3.6 Ma in the Tejon depocenter and 3.2 to 3.5 Ma in the Northern Buttonwillow depocenter (table 12.2), most of the oil was expelled in the last 0.6 Ma (fig. 12.16). On the basis of the present-day (0 Ma) time-slice map, most oil expelled from the Antelope shale source rock originated in the Tejon depocenter, although significant quantities of this oil also originated in the Northern and Southern Buttonwillow depocenters (fig. 12.16).

The 4-D model predicts that most oil was generated from the Kreyenhagen Formation source rock since 3 Ma (fig 12.17). Little oil generated from the Kreyenhagen Formation originated from the Tejon depocenter because the source rock is thin or absent there. However, significant volumes of oil originated from the Kreyenhagen Formation source rock in the Southern Buttonwillow, and especially the Northern Buttonwillow depocenters. The 0 Ma time-slice map shows that the Kreyenhagen Formation is overmature in the deepest portions of the Northern Buttonwillow depocenter (fig. 12.17).

The 4-D model predicts that the Moreno Formation source rock had already expelled light oil in an area immediately southeast of the Jacalitos field about 52 Ma (fig. 12.18). On the basis of a 1-D extraction in the center of this area, initial, peak, and end of oil expulsion occurred at 58, 54, and 46 Ma, respectively (table 12.2). (Figure 12.18 depicts the amount of expelled oil at 52 Ma rather than 58 Ma because the areal extent of expelled oil for the latter time is limited and not readily seen at the scale of the figure.) In contrast, the 4-D model shows that petroleum expulsion from the Moreno Formation continues to present day in other locations. Significant amounts of light oil originated from the Moreno Formation since 6 Ma east of the Jacalitos field (fig. 12.18), but none of this oil has been identified in existing fields to date. It is possible that light oil generated from the Moreno Formation in the area near Jacalitos field may have accumulated, but was later flushed out of traps by subsequent gases generated from the Moreno Formation or by oil generated from the Kreyenhagen Formation.

Previous work suggested that the distal shales of the Late Cretaceous Winters formation of Edmondson (1962) in the Sacramento Basin generated hydrocarbon gases that migrated to traps in the northern San Joaquin Basin prior to formation of the Stockton Arch (as discussed in Magoon and others, this volume, chapter 8, and in Hosford Scheirer and Magoon, this volume, chapter 21). On the basis of our 4-D model results, the Moreno Formation in the San Joaquin Basin may have generated gas that subsequently migrated into the gas fields in the northern part of the basin. The 4-D model shows that potential migration flow lines lie stratigraphically above and below the Moreno Formation and are directed toward those fields.

The results of our 4-D petroleum systems model confirm many source rock-reservoir rock relationships observed in the San Joaquin Basin Province, indicating that the model captures the salient features of the petroleum systems in the basin. For example, production data suggest that significant amounts of petroleum generated from the Antelope shale migrated downward into the Temblor Formation where it was trapped; this scenario was also observed in the 4-D model. Production data also indicate that much of the oil and associated gas generated from the Antelope shale was trapped in the Stevens sand encased within the source rock (see tables in Magoon and others, this volume, chapter 8). Petroleum occurrences demonstrate that the complex depositional system of the Stevens sand (Webb, 1981) interbedded within the Antelope

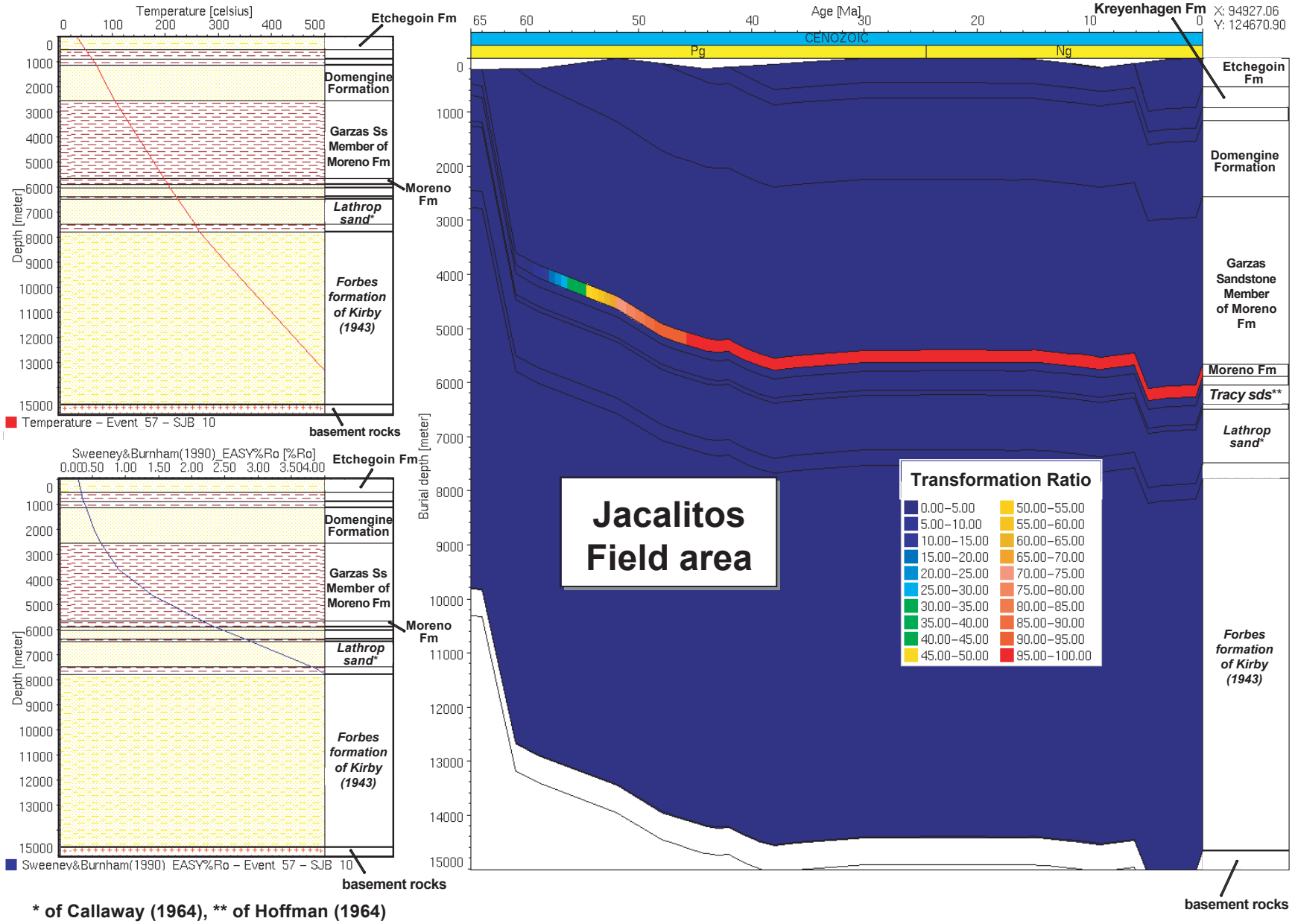

Figure 12.15. One-dimensional (1-D) burial-history model extracted from immediately southeast of the Jacalitos field (yellow patch, figure 12.18 at 52 Ma) shows calculated temperature (top left), vitrinite reflectance (bottom left), and transformation ratio (percent, right) for the Moreno Formation source rock. On the basis of the transformation ratio plot, the Moreno Formation source rock began to expel petroleum (10-percent transformation ratio) about 58 Ma, reached peak expulsion (50-percent transformation ratio) about 54 Ma, and reached the end of oil expulsion (95-percent transformation ratio) about 46 Ma (table 12.2) at this location. Formation names in italics are informal. Fm, Formation; sds, sands.

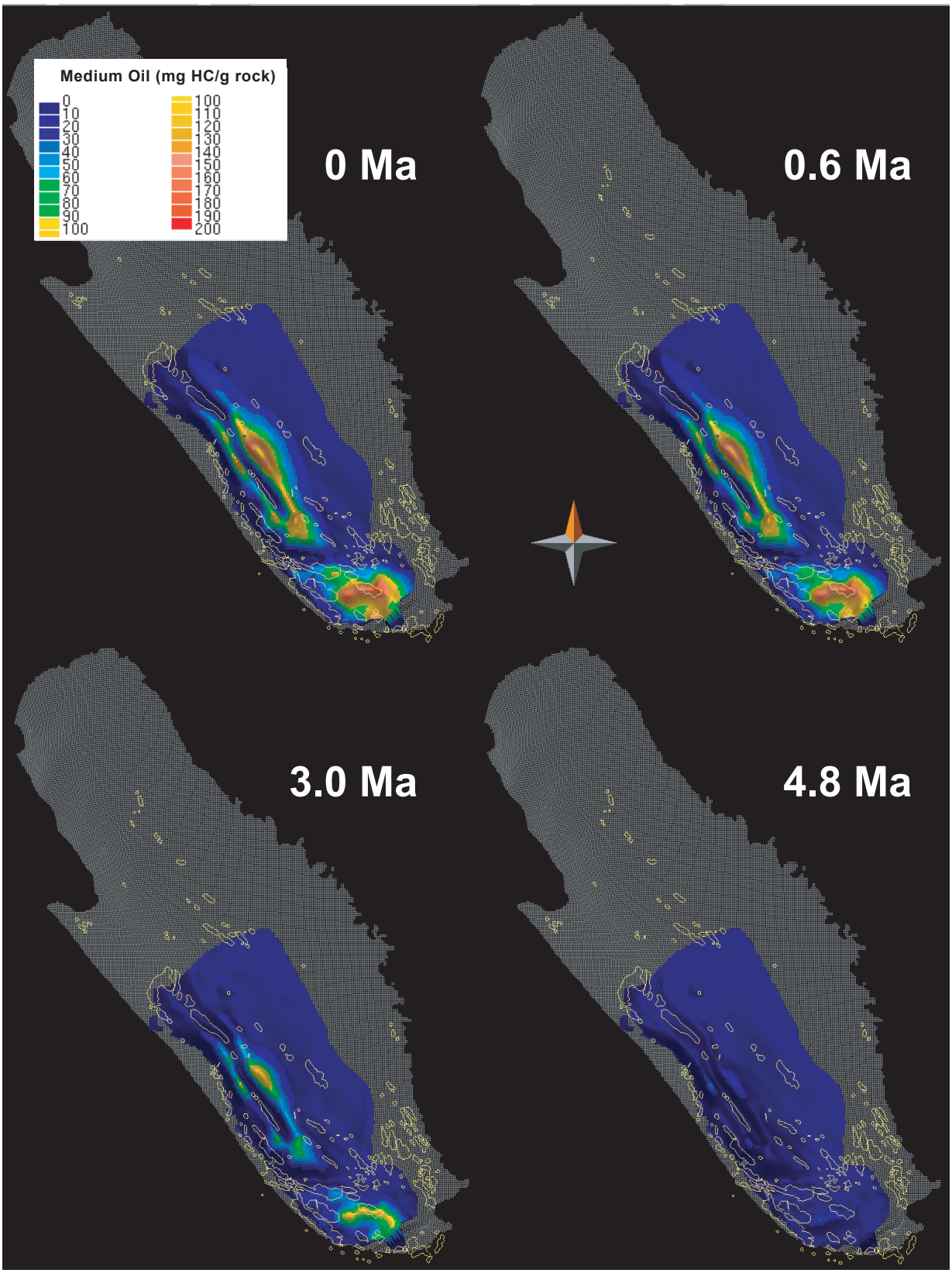

Figure 12.16. Maps of the calculated amounts of medium oil (25 to 35 degrees API gravity) generated from the upper part of the Antelope shale (mg hydrocarbon/g rock) at 0 Ma (present day), 0.6 Ma, 3.0 Ma, and 4.8 Ma.

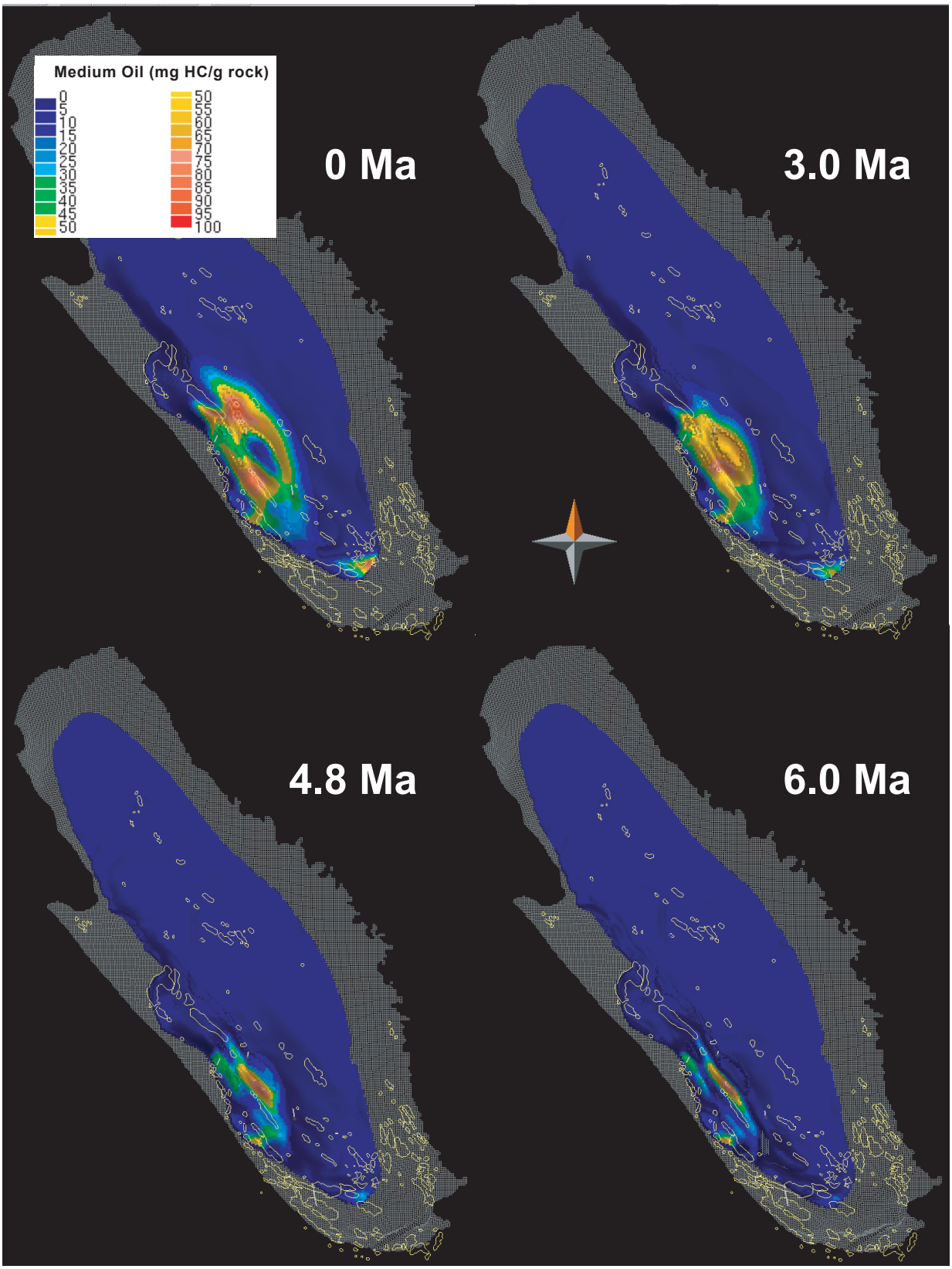

Figure 12.17. Maps of the calculated amounts of medium oil (25 to 35 degrees API gravity) generated from the Kreyenhagen Formation (mg hydrocarbon/g rock) at 0 Ma (present day), 3.0 Ma, 4.8 Ma, and 6.0 Ma. Note that the color scale extends to only 100 mg hydrocarbon/g rock compared to 200 mg hydrocarbon/g rock in the Antelope shale figure (fig. 12.16). A value of zero for expelled oil in the center of the present-day Northern Buttonwillow depocenter indicates that the Kreyenhagen Formation source rock is overmature in that location.

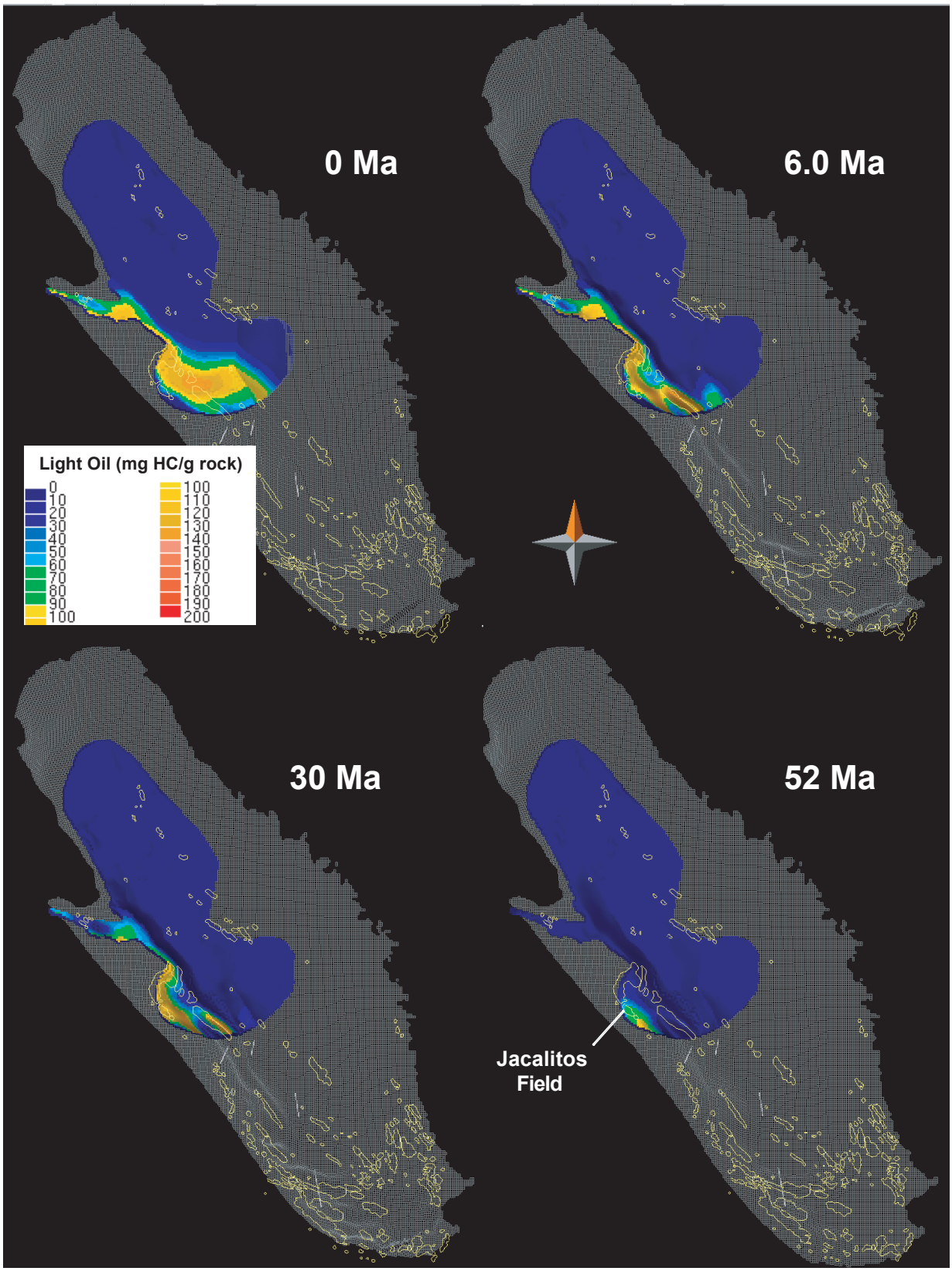

Figure 12.18. Maps of the calculated amounts of light oil (35 to 45 degrees API gravity) generated from the Moreno Formation (mg hydrocarbon/g rock) at 0 Ma (present day), 6.0 Ma, 30 Ma, and 52 Ma.

shale source rock provides ample conduits for oil migration. Submarine braided channels and feeder systems are highly interconnected, suggesting that most potential reservoir lithologies within the Stevens sand were exposed to petroleum charge. The numerous oil fields that produce from the Stevens sand at the lower end of the Bakersfield Arch are proof of this connectivity. Our 4-D model shows that petroleum generated from the Antelope shale migrated into the Stevens sand as well as updip into shallower and younger reservoir rocks.

The 4-D model predicts the orientation of petroleum migration pathways away from pods of active source rock. For example, petroleum generated from the Antelope shale in the Tejon depocenter migrates to the northwest into the Paloma field, where it fills the trap to spill point and is then diverted to the northeast along the Bakersfield Arch toward Kern River field (fig. 12.19). The figure also shows that the anticlinal trap at the Lost Hills field receives petroleum from both the Northern and Southern Buttonwillow depocenters to the northeast and southeast, respectively (fig. 12.19).

The 4-D model also provides valuable insights on the source of crude oil in newly discovered fields in the San Joaquin Basin. Significant volumes of oil occur in shallow fractured Antelope shale source rock in this basin. Many industry geologists conclude that these accumulations represent locally generated petroleum, particularly in certain recently discovered fields where accumulations appear to be controlled by the transition from the opal CT to quartz facies of silica. For example, silica diagenesis is the trapping mechanism for accumulations of petroleum in the Rose and North Shafter fields (Grau and others, 2003). However, the 22^{o} API gravity oils from these fields are thermally mature. Our 4-D model shows that the Antelope shale and associated reservoir rock facies near the Rose and North Shafter fields are thermally immature. Thus, we conclude that these accumulated oils migrated eastward from more deeply buried, thermally mature Antelope shale source rock into reservoir rock within the McLure Shale. Kruge (1986) reached similar conclusions. On the basis of biomarker evidence, he found that the thermal maturity of oils produced from Antelope shale reservoirs was too high for the oils to have originated in place. Kruge (1986) concluded that at least 4 km (about 13,000 ft) of burial was required for generation of oil in the Antelope shale.

As discussed earlier in this paper, the 4-D model of the San Joaquin Basin Province contains generalized input that precludes comparisons of the results on a field-by-field basis. Nevertheless, a map of accumulations predicted by the model for one area within the basin (fig. 12.20) compares reasonably well with the locations of known fields. A cross-section of the model shows that the petroleum generated by the model fills large structural traps, such as that in the Lost Hills field (fig. 12.21). However, complex stratigraphic or combination traps are difficult to model without more detailed geologic information than was available for this study. Note that some known fields in figure 12.20 lack corresponding modeled accumulations, whereas some modeled accumulations occur in locations without known fields. In addition, the model is unable to predict many fields with dimensions that approach model resolution (1 km).

Conclusions

Our 4-D petroleum systems model helps to explain the distribution of petroleum accumulations within the San Joaquin Basin Province. The 4-D model results indicate that petroleum accumulations originate mainly from the Antelope shale in the south and the Kreyenhagen Formation or Moreno Formation toward the north. The Tejon depocenter in the southern part of the study area is somewhat more favorable for generation of Antelope shale petroleum than the Southern and Northern Buttonwillow depocenters to the north, mainly due to thicker accumulations of Antelope shale source rock (table 12.2). The Tejon and Southern Buttonwillow depocenters contain similar, favorable amounts of oil-prone Type II or Type IIS organic matter (about 2.0 to 5.5 weight percent total organic carbon; 300 to 400 mg hydrocarbon/g total organic carbon), whereas the quantity and quality of Antelope shale organic matter is less favorable in the Northern Buttonwillow depocenter (1.0 to 2.0 weight percent total organic carbon; 200 to 350 mg hydrocarbon/g total organic carbon).

On the basis of our 4-D petroleum systems model, virtually all petroleum generation from the Antelope shale source rock within the San Joaquin Basin occurred since 5 Ma (Pliocene to Holocene; table 12.2). The timing of peak expulsion from Antelope shale source rock is similar in the Tejon (3.6 Ma) and Northern Buttonwillow depocenters (3.2 to 3.5 Ma), but occurred much later in the Southern Buttonwillow depocenter (0.5 to 1.0 Ma). Antelope shale source rock has not reached the end of oil expulsion in any of these three depocenters, although it is highly mature in the deepest portions of the Tejon and Northern Buttonwillow depocenters. In the deepest portion of the Southern Buttonwillow depocenter, the Antelope shale source rock has only reached 52 to 56 percent transformation ratio. Magoon and others (this volume, chapter 8) discuss the favorable timing of these petroleum generation events compared to the timing of late Tertiary structural and stratigraphic traps in the basin.

In contrast to the Antelope shale, the Kreyenhagen Formation source rock is thicker and generally contains more favorable quantities and quality of organic matter to the north of the Tejon depocenter. Kreyenhagen Formation source rock is thin or absent in the Tejon depocenter (table 12.2). The most favorable quantities (2.0 to 3.0 weight percent) and quality (350 to 450 mg hydrocarbon/g total organic carbon) of Kreyenhagen Formation organic matter occur in the Northern Buttonwillow depocenter. Peak expulsion from Kreyenhagen Formation source rock in the Northern Buttonwillow depocenter occurred about 4.3 Ma and the source rock in the deepest part of the depocenter reached the end of oil expulsion about 3.6 Ma. Although similar in thickness to the Kreyenhagen Formation in the Northern Buttonwillow depocenter, the Antelope shale source rock generally contains less organic matter that is

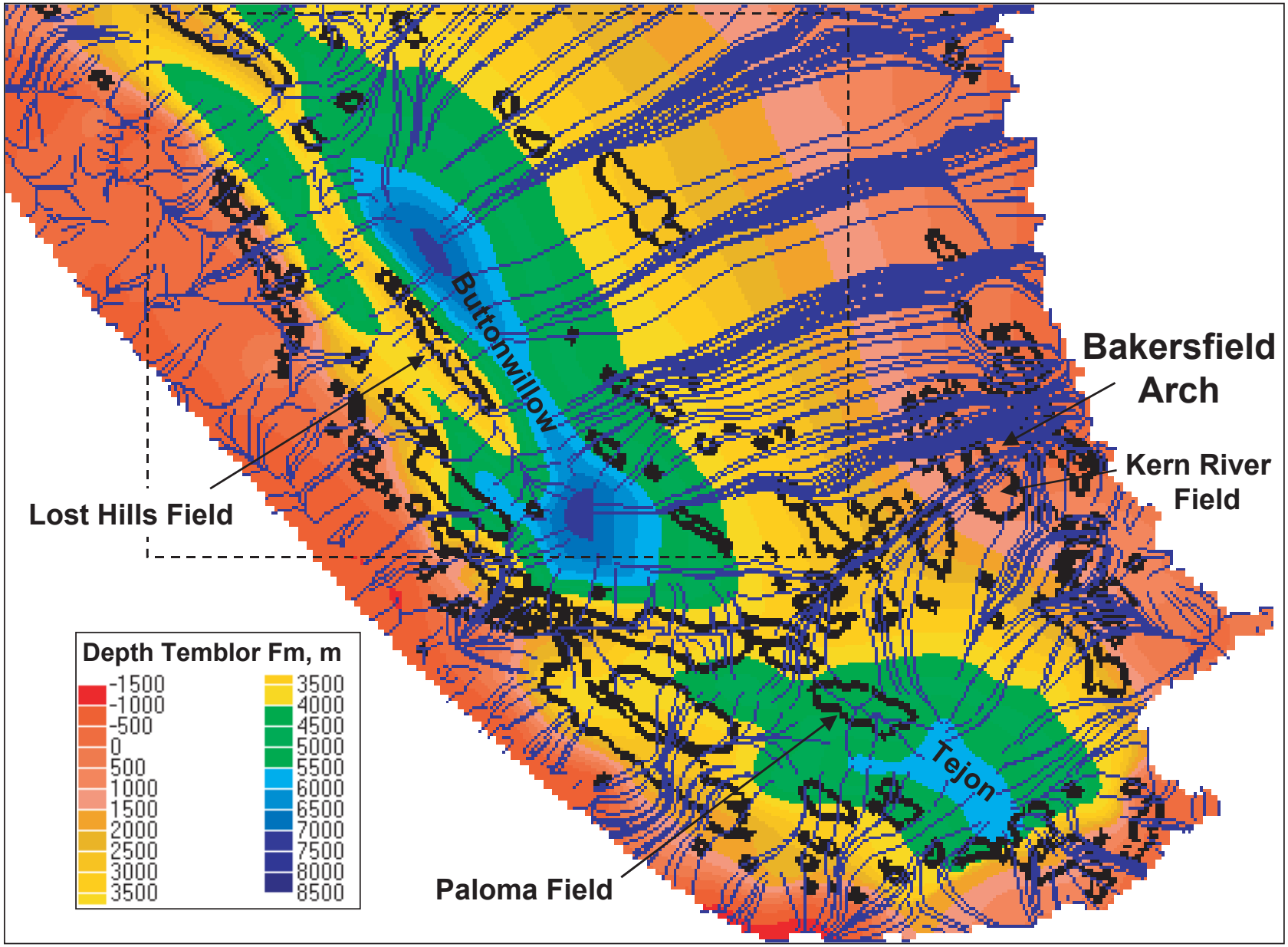

Figure 12.19. Map shows potential migration pathways (blue lines), mainly within the Temblor Formation, for petroleum generated from the Antelope shale and Kreyenhagen Formation in the Tejon and Buttonwillow depocenters. Positive and negative depth values (inset) indicate depth below or elevation above sea level, respectively. To simplify the pathways in the figure, sealing faults and stratigraphic traps were removed for this view. The dashed box indicates the location of a map showing oil and gas accumulations predicted by the four-dimensional (4-D) model (fig. 12.20). Fm, Formation; m, meters.

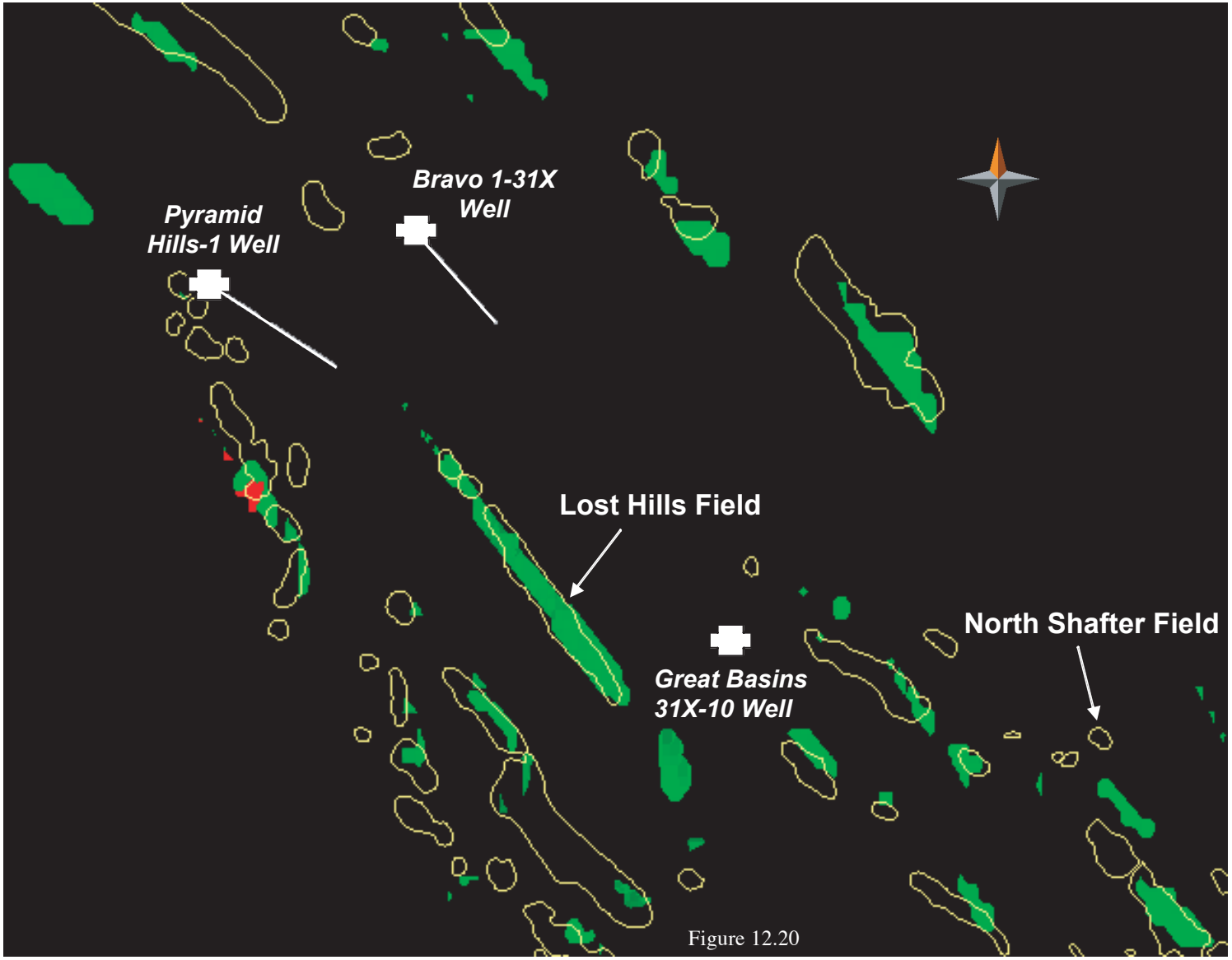

Figure 12.20. The four-dimensional (4-D) petroleum systems model predicts oil (green) and gas (red) accumulations in a selected area of the San Joaquin Basin Province (see fig. 12.19) that compare reasonably well with outlines of known fields (yellow boundaries). The three wells (white crosses) were drilled vertically. However, because the figure is a view downward into a three-dimensional model from near the location of the Great Basins 31X-10 well, the drilled intervals for the other wells appear as inclined white lines from the surface to total depth. The accumulations are at various depths in the model, whereas the field outlines were projected to the surface. The model does not accurately predict many fields with dimensions that approach model resolution (1 km).

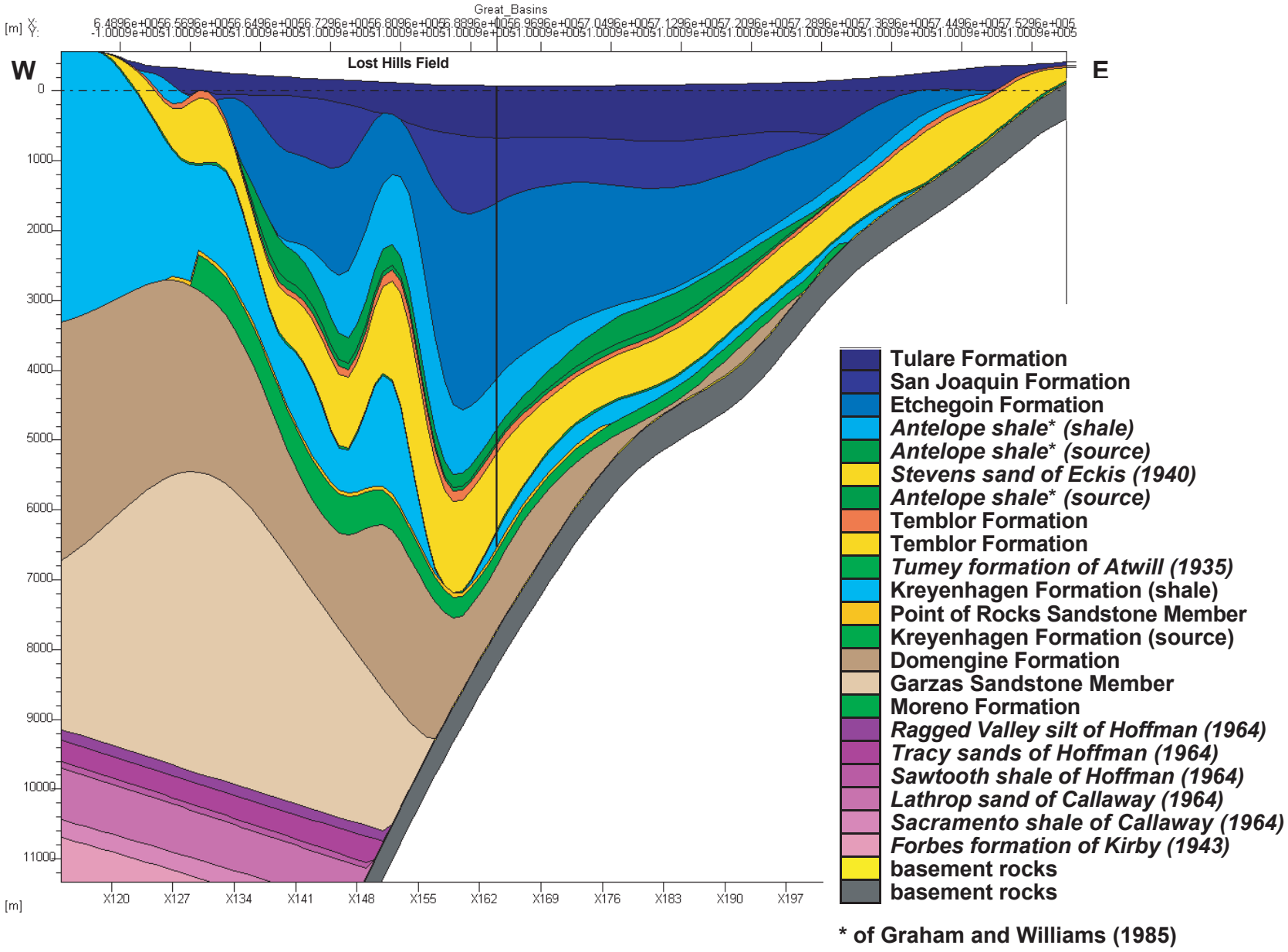

Figure 12.21. East-west cross-section through the four-dimensional (4-D) model at Great Basins 31X-10 well shows anticlinal closures that trap oil in Antelope shale, Tembor Formation, and Point of Rocks Sandstone Member reservoirs in the Lost Hills field (fig. 12.20). The 4-D model predicts that most oil generated from thermally mature Antelope shale and Kreyenhagen Formation source rocks in the syncline to the east of the field migrates to the west into the field or to the east until it accumulates in stratigraphic traps or escapes to the surface. Formation names in italics are informal.

of lower quality. Furthermore, the Antelope shale source rock has not reached the end of oil expulsion in the deepest parts of the Northern Buttonwillow depocenter (83 to 87 percent transformation ratio), suggesting that more petroleum originates from the Kreyenhagen Formation source rock (100 percent transformation ratio) at this location.

The Moreno Formation source rock in the area to the south of the Jacalitos field is thick and organic-rich, similar to the Kreyenhagen Formation in the nearby Northern Buttonwillow depocenter. However, the Moreno Formation source rock at this location expelled petroleum (58 Ma; table 12.2) and reached the end of oil expulsion (46 Ma) in Paleocene to Eocene time, which was much earlier than nearby Kreyenhagen Formation source rock in the Northern Buttonwillow depocenter (5.5 Ma and 3.6 Ma, respectively). The 4-D model shows that petroleum expulsion from the Moreno Formation continues to present-day in other locations. Significant amounts of light oil originated from the Moreno Formation since 6 Ma, mainly to the east of the Jacalitos field (fig. 12.18).

Oil accumulations that can be attributed to the Moreno Formation source rock are rare, possibly because they were lost or destroyed since the time of emplacement or because the oil was displaced or diluted by later-generated Moreno Formation hydrocarbon gas or oil from the Kreyenhagen Formation source rock. Nonetheless, some of the gas in accumulations in the northern San Joaquin Basin may originate from Moreno Formation source rock rather than distal shales of the Winters formation of Edmondson (1962) in the Sacramento Valley.

Acknowledgments

We thank Cari Johnson (University of Utah), Steve Graham (Stanford University), and Tor Nilsen (consulting geologist) for geologic input. Colin Williams provided surface heat-flow data that were used to construct our surface heat-flow map. Bonnie Bloeser (AERA Energy LLC), Janet Pitman, Charles Powell II, Jim Hendley, and Jim Schmoker provided useful reviews of the draft paper. We thank Don Gautier and Chris Schenk for recognizing the utility of petroleum systems models to assist in petroleum resource assessment. We especially thank Dave Fowler and Tony Steele (Occidental Petroleum) for useful discussions. “EarthVision” is a registered trademark (Marca Registrada) of Dynamic Graphics, Inc. “PetroMod” is a registered trademark (Marca Registrada) of IES GmbH (Integrated Exploration Systems).

References Cited

Atwater, T., 1970, Implications of plate tectonics for the Cenozoic tectonic evolution of western North America: Geological Society of America Bulletin, v. 81, no. 12, p. 3513-3535.

Atwill, E.R., 1935, Oligocene Tumey Formation of California: Bulletin of the American Association of Petroleum Geologists, v. 19, no. 8, p. 1192-1204.

Aziz, K., and Settari, A., 1979, Petroleum reservoir simulation: London, Applied Science Publishers, 476 p.

Bandy, O.L., and Arnal, R.E., 1969, Middle Tertiary basin development, San Joaquin Valley, California: Geological Society of America Bulletin, v. 80, no. 5, p. 783-819.

Bartow, J.A., and McDougall, K., 1984, Tertiary stratigraphy of the southeastern San Joaquin Valley, California: U.S. Geological Survey Bulletin 1529-J, 41 p.

Baskin, D.K., and Peters, K.E., 1992, Early generation characteristics of a sulfur-rich Monterey kerogen: American Association of Petroleum Geologists Bulletin, v. 76, no. 1, p. 1-13.

Behar, F., Vandenbroucke, M., Tang, Y., Marquis, F., and Espitalie, J., 1997, Thermal cracking of kerogen in open and closed systems—Determination of kinetic parameters and stoichiometric coefficients for oil and gas generation: Organic Geochemistry, v. 26, no. 5-6, p. 321-339.

Beyer, L.A., and Bartow, J.A., 1987, Summary of geology and petroleum plays used to assess undiscovered recoverable petroleum resources, San Joaquin Basin Province, California: United States Geological Survey Open-File Report 87-450Z, 80 p.

Bishop, C.C., 1970, Upper Cretaceous stratigraphy on the west side of the Northern San Joaquin Valley, Stanislaus and San Joaquin counties, California: Sacramento, Calif., California Division of Mines and Geology Special Report 104, 29 p.

Bloch, R.B., 1991, Studies of the stratigraphy and structure of the San Joaquin Basin, California: Stanford, Calif., Stanford University, Ph.D. dissertation, 319 p.

Callaway, D.C., 1964, Distribution of uppermost Cretaceous sands in the Sacramento-Northern San Joaquin Basin of California: Selected Papers Presented to San Joaquin Geological Society, v. 2, p. 5-18.

Callaway, D.C., 1971, Petroleum potential of San Joaquin Basin, California, *in* Cram, I.H., ed., Future petroleum provinces of the United States—Their geology and potential: Tulsa, Okla., American Association of Petroleum Geologists Memoir 15, p. 239-253.

Callaway, D.C., 1990, Organization of stratigraphic nomenclature for the San Joaquin Basin, California, *in* Kuespert, J.G., and Reid, S.A., eds., Structure, stratigraphy, and hydrocarbon occurrences of the San Joaquin Basin, California: Bakersfield, Calif., Pacific Sections, Society of Economic Paleontologists and Mineralogists and American Association of Petroleum Geologists, v. 64, p. 5-21.

Eckis, R., 1940, The Stevens sand, southern San Joaquin Valley, California [abs.]: Bulletin of the American Association of Petroleum Geologists, v. 24, no. 12, p. 2195-2196.

Edmondson, W.F., 1962, Stratigraphy of the late Upper Cretaceous in the Sacramento Valley: Selected Papers Presented to San Joaquin Geological Society, v. 1, p. 17-26.

Edwards, E.C., 1943, Kern Front area of the Kern River oil field, *in* Jenkins, O.P., ed., Geologic formations and

economic development of the oil and gas fields of California: San Francisco, State of California, Department of Natural Resources, Division of Mines Bulletin No. 118, p. 571-574.

Fonseca-Rivera, C., 1998, Late Cretaceous-early Tertiary paleoceanography and cyclic sedimentation along the California margin—Evidence from the Moreno Formation: Stanford, Calif., Stanford University, Ph.D. dissertation, 449 p.

Gautier, D.L., Hosford Scheirer, A., Tennyson, M.E., Peters, K.E., Magoon, L.B., Lillis, P.G., Charpentier, R.R., Cook, T.A., French, C.D., Klett, T.R., Pollastro, R.M., and Schenk, C.J., 2004, Assessment of Undiscovered Oil and Gas Resources of the San Joaquin Basin Province of California, 2003: U.S. Geological Survey Fact Sheet FS-2004-0343 [also available at URL http://pubs.usgs.gov/fs/2004/3043/].

Goudkoff, P.P., 1943, Correlation of oil field formations on west side of San Joaquin Valley, *in* Jenkins, O.P., ed., Geologic formations and economic development of the oil and gas fields of California: San Francisco, State of California, Department of Natural Resources, Division of Mines Bulletin No. 118, p. 247-252.

Graham, S.A., and Williams, L.A., 1985, Tectonic, depositional, and diagenetic history of Monterey Formation (Miocene), central San Joaquin Basin, California: American Association of Petroleum Geologists Bulletin, v. 69, no. 3, p. 385-411.

Grau, A., Kidney, R., and Sterling, R., 2003, Success! Using seismic attributes and horizontal drilling to delineate and exploit a diagenetic trap, Monterey Shale, San Joaquin Valley, California: Search and Discovery Article, no. 20011 [available at http://www.searchanddiscovery.com/documents/2003/grau/index.htm].

Gropp, W., Ewing, L., and Sterling, T., 2003, Beowulf cluster computing with Linux, Second edition: Cambridge, Mass., MIT Press, 504 p.

Hantschel, T., Kauerauf, A.I., and Wygrala, B., 2000, Finite element analysis and ray tracing modeling of petroleum migration: Marine and Petroleum Geology, v. 17, no. 7, p. 815-820.

Hoffman, R.D., 1964, Geology of the northern San Joaquin Valley: Selected Papers Presented to San Joaquin Geological Society, v. 2, p. 30-45.

Jarvie, D.M., Claxton, B.L., Henk, F.B., and Breyer, J.T., 2001, Oil and shale gas from the Barnett Shale, Ft. Worth Basin, Texas [abs.]: American Association of Petroleum Geologists Bulletin, v. 85, p. A100.

Jarvie, D.M., and Lundell, L.L., 2001, Kerogen type and thermal transformation of organic matter in the Miocene Monterey Formation, *in* Isaacs, C.M., and Rullkötter, J., eds., The Monterey Formation—From rocks to molecules: New York, Columbia University Press, p. 268-295.

Kasline, F.E., 1942, Edison oil field, *in* Summary of operations, California oil fields: San Francisco, Annual Report of the State Oil and Gas Supervisor, v. 26, p. 12-18 [also available *in* California Division of Oil and Gas, Summary of Operations, 1915-1999: California Division of Conservation, Division of Oil, Gas, and Geothermal Resources, Publication No. CD-3, and at ftp://ftp.consrv.ca.gov/pub/oil/Summary_of_Operations/1940/].

Kirby, J.M., 1943, Upper Cretaceous stratigraphy of the west side of Sacramento Valley south of Willows, Glenn County, California: Bulletin of the American Association of Petroleum Geologists, v. 27, no. 3, p. 279-305.

Kruge, M.A., 1986, Biomarker geochemistry of the Miocene Monterey Formation, West San Joaquin Basin, California—Implications for petroleum generation: Organic Geochemistry, v. 10, no. 1-3, p. 517-530.

Lewan, M.D., 1987, Petrographic study of primary petroleum migration in the Woodford Shale and related rock units, *in* Doligez, B., ed., Migration of hydrocarbons in sedimentary basins: Paris, Éditions Technip, p. 113-130.

Lillis, P.G., and Magoon, L.B., 2004, Oil-oil correlation to establish a basis for mapping petroleum systems, San Joaquin Basin, California: U.S. Geological Survey Open-File Report 2004-1037, 42 p. [http://pubs.usgs.gov/of/2004/1037].

Loken, K.P., 1959, Gill Ranch gas field, *in* Summary of operations, California oil fields: San Francisco, Annual Report of the State Oil and Gas Supervisor, v. 45, no. 1, p. 27-32 [also available *in* California Division of Oil and Gas, Summary of Operations, 1915-1999: California Division of Conservation, Division of Oil, Gas, and Geothermal Resources, Publication No. CD-3, and at ftp://ftp.consrv.ca.gov/pub/oil/Summary_of_Operations/1959/].

Magoon, L.B., and Dow, W.G., 1994, The petroleum system, *in* Magoon, L.B., and Dow, W.G., eds., The petroleum system—From source to trap: Tulsa, Okla., American Association of Petroleum Geologists Memoir 60, p. 3-24.

McMasters, J.H., 1948, Oceanic sand [abs.]: Bulletin of the American Association of Petroleum Geologists, v. 32, no. 12, p. 2320.

Miller, R.H., and Bloom, C.V., 1939, Mountain View oil field, *in* Summary of operations, California oil fields: San Francisco, Annual Report of the State Oil and Gas Supervisor, v. 22, no. 4, p. 5-36 [also available *in* California Division of Oil and Gas, Summary of Operations, 1915-1999: California Division of Conservation, Division of Oil, Gas, and Geothermal Resources, Publication No. CD-3, and at ftp://ftp.consrv.ca.gov/pub/oil/Summary_of_Operations/1937/].

Noble, E.B., 1940, Rio Bravo oil field, Kern County, California: Bulletin of the American Association of Petroleum Geologists, v. 24, no. 7, p. 1330-1333.

Orr, W.L., 1986, Kerogen/asphaltene/sulfur relationships in sulfur-rich Monterey oils: Organic Geochemistry, v. 10, no. 1-3, p. 499-516.

Peters, K.E., and Cassa, M.R., 1994, Applied source rock geochemistry, *in* Magoon, L.B., and Dow, W.G., eds., The petroleum system—From source to trap: Tulsa, Okla., American Association of Petroleum Geologists Memoir 60, p. 93-117.

Peters, K.E., Moldowan, J.M., and Sundararaman, P., 1990, Effects of hydrous pyrolysis on biomarker thermal maturity parameters—Monterey phosphatic and siliceous members: Organic Geochemistry, v. 15, no. 3, p. 249-265.

Peters, K.E., Pytte, M.H., Elam, T.D., and Sundararaman, P., 1994, Identification of petroleum systems adjacent to the San Andreas Fault, California, USA, *in* Magoon, L.B., and Dow, W.G., eds., The petroleum system—From source to trap: Tulsa, Okla., American Association of Petroleum Geologists Memoir 60, p. 423-436.

Peters, K.E., Walters, C.C., and Moldowan, J.M., 2005, The biomarker guide: Cambridge, U.K., Cambridge University Press, 1155 p.

PS-AAPG, 1957a, Cenozoic correlation section across south San Joaquin Valley from San Andreas Fault to Sierra Nevada foot hills: Pacific Section, American Association of Petroleum Geologists, prepared by the San Joaquin Valley Sub-committee on the Cenozoic of the Geologic Names and Correlation Committee of the American Association of Petroleum Geologists (Church, H. V., Jr. and Krammes, K., co-chairmen), Section 8, 1 sheet.

PS-AAPG, 1957b, Correlation section across central San Joaquin Valley from San Andreas fault to Sierra Nevada foot hills, California: Pacific Section, American Association of Petroleum Geologists, prepared by the San Joaquin Valley Sub-committee on the Cenozoic of the Geologic Names and Correlation Committee of the American Association of Petroleum Geologists (Church, H. V., Jr. and Krammes, K., co-chairmen), Section 9, 1 sheet.

PS-AAPG, 1958a, Correlation section longitudinally north-south through central San Joaquin Valley from Rio Vista through Riverdale (10 north) and Riverdale through Tejon Ranch area (10 south), California: Pacific Section, American Association of Petroleum Geologists, prepared by the San Joaquin Valley Sub-committee on the Cenozoic of the Geologic Names and Correlation Committee of the American Association of Petroleum Geologists (Church, H. V., Jr. and Krammes, K., co-chairmen), Section 10N, 1 sheet.

PS-AAPG, 1958b, Correlation section longitudinally north-south through central San Joaquin Valley from Rio Vista through Riverdale (10 north) and Riverdale through Tejon Ranch area (10 south), California: Pacific Section, American Association of Petroleum Geologists, prepared by the San Joaquin Valley Sub-committee on the Cenozoic of the Geologic Names and Correlation Committee of the American Association of Petroleum Geologists (Church, H. V., Jr. and Krammes, K., co-chairmen), Section 10S, 1 sheet.

PS-AAPG, 1959, Correlation section longitudinally north-south through Coalinga to Midway Sunset and across San Andreas Fault into southeast Cuyama Valley, California: Pacific Section, American Association of Petroleum Geologists, prepared by the San Joaquin Valley Sub-committee on the Cenozoic of the Geologic Names and Correlation Committee of the American Association of Petroleum Geologists (Church, H. V., Jr. and Krammes, K., co-chairmen), Section 11, 1 sheet.

PS-AAPG, 1989, Correlation section no. 27 through central San Joaquin Valley from Turk Anticline (Cantua Creek) to the Transverse Range, Fresno, King and Kern counties, California: Pacific Section, American Association of Petroleum Geologists, prepared by the San Joaquin Valley Sub-committee on the Cenozoic of the Geologic Name Correlation Committee of the American Association of Petroleum Geologists (Villanueva, L. and Kappeler, J., chairmen), 1 sheet.

Reid, S.A., 1995, Miocene and Pliocene depositional systems of the southern San Joaquin basin and formation of sandstone reservoirs in the Elk Hills area, California, *in* Fritsche, A.E., ed., Cenozoic paleogeography of the western United States—II: Pacific Section, Society of Economic Paleontologists and Mineralogists, p. 131-150.

Sass, J.H., Lachenbruch, A.H., Munroe, R.J., Greene, G.W., and Moses, T.H., Jr., 1971, Heat flow in the western United States: Journal of Geophysical Research, v. 76, no. 26, p. 6376-6413.

Sullivan, J.C., 1963, Guijarral Hills oil field, *in* Summary of operations, California oil fields: San Francisco, Annual Report of the State Oil and Gas Supervisor, v. 48, no. 2, p. 37-51 [also available *in* California Division of Oil and Gas, Summary of Operations, 1915-1999: California Division of Conservation, Division of Oil, Gas, and Geothermal Resources, Publication No. CD-3, and at ftp://ftp.consrv.ca.gov/pub/oil/Summary_of_Operations/1962/].

Sweeney, J., and Burnham, A.K., 1990, Evaluation of a simple model of vitrinite reflectance based on chemical kinetics: American Association of Petroleum Geologists Bulletin, v. 74, no. 10, p. 1559-1570.

Teichmüller, M., and Durand, B., 1983, Fluorescence microscopical rank studies on liptinites and vitrinites in peat and coals, and comparison with results of the Rock-Eval pyrolysis: International Journal of Coal Geology, v. 2, no. 3, p. 197-230.

Webb, G.W., 1981, Stevens and earlier Miocene turbidite sandstones, southern San Joaquin Valley, California: American Association of Petroleum Geologists Bulletin, v. 65, p. 438-465.

Welte, D.H., Horsfield, B., and Baker, D.R., eds., 1997, Petroleum and basin evolution: New York, Springer-Verlag, 535 p.

Wentworth, C.M., Fisher, G.R., Levine, P., and Jachens, R.C., 1995, The surface of crystalline basement, Great Valley and Sierra Nevada, California—A digital map database: U.S. Geological Survey Open-File Report 95-96, 16 p.

Wilkinson, E.R., 1960, Vallecitos field, *in* Summary of operations, California oil fields: San Francisco, Annual Report of the State Oil and Gas Supervisor, v. 45, no. 2, p. 17-33 [also available *in* California Division of Oil and Gas, Summary of Operations, 1915-1999: California Division of Conservation, Division of Oil, Gas, and Geothermal Resources, Publication No. CD-3, and at ftp://ftp.consrv.

ca.gov/pub/oil/Summary_of_Operations/1959/].
Wygrala, B.P., 1989, Integrated study of an oil field in the southern Po Basin, Northern Italy: West Germany, University of Cologne, Ph.D. dissertation, 217 p.
Zienkiewicz, O.C., 1977, The finite element method: London, McGraw-Hill, 787 p.